



**University of
Zurich**^{UZH}

**Zurich Open Repository and
Archive**

University of Zurich
Main Library
Strickhofstrasse 39
CH-8057 Zurich
www.zora.uzh.ch

Year: 2021

Analysis of genomic DNA from medieval plague victims suggests long-term effect of *Yersinia pestis* on human immunity genes

Immel, Alexander ; Key, Felix M ; Szolek, András ; et al ; Schuenemann, Verena J ; Reiter, Ella

Abstract: Pathogens and associated outbreaks of infectious disease exert selective pressure on human populations, and any changes in allele frequencies that result may be especially evident for genes involved in immunity. In this regard, the 1346-1353 *Yersinia pestis*-caused Black Death pandemic, with continued plague outbreaks spanning several hundred years, is one of the most devastating recorded in human history. To investigate the potential impact of *Y. pestis* on human immunity genes we extracted DNA from 36 plague victims buried in a mass grave in Ellwangen, Germany in the 16th century. We targeted 488 immune-related genes, including HLA, using a novel in-solution hybridization capture approach. In comparison with 50 modern native inhabitants of Ellwangen, we find differences in allele frequencies for variants of the innate immunity proteins Ficolin-2 and NLRP14 at sites involved in determining specificity. We also observed that HLA-DRB1*13 is more than twice as frequent in the modern population, whereas HLA-B alleles encoding an isoleucine at position 80 (I-80+), HLA C*06:02 and HLA-DPB1 alleles encoding histidine at position 9 are half as frequent in the modern population. Simulations show that natural selection has likely driven these allele frequency changes. Thus, our data suggests that allele frequencies of HLA genes involved in innate and adaptive immunity responsible for extracellular and intracellular responses to pathogenic bacteria, such as *Y. pestis*, could have been affected by the historical epidemics that occurred in Europe.

DOI: <https://doi.org/10.1093/molbev/msab147>

Posted at the Zurich Open Repository and Archive, University of Zurich

ZORA URL: <https://doi.org/10.5167/uzh-203424>

Journal Article

Accepted Version

Originally published at:

Immel, Alexander; Key, Felix M; Szolek, András; et al; Schuenemann, Verena J; Reiter, Ella (2021). Analysis of genomic DNA from medieval plague victims suggests long-term effect of *Yersinia pestis* on human immunity genes. *Molecular Biology and Evolution*, 38(10):4059-4076.

DOI: <https://doi.org/10.1093/molbev/msab147>

Analysis of genomic DNA from medieval plague victims suggests long-term effect of *Yersinia pestis* on human immunity genes

Alexander Immel^{1,2,3}, Felix M. Key^{1,4*}, András Szolek^{5*}, Rodrigo Barquera^{1*}, Madeline K. Robinson⁶, Genelle F. Harrison⁶, William H. Palmer⁶, Maria A. Spyrou^{1,3}, Julian Susat², Ben Krause-Kyora², Kirsten I. Bos^{1,3}, Stephen Forrest³, Diana I. Hernández-Zaragoza^{1,7}, Jürgen Sauter⁸, Ute Solloch⁸, Alexander H. Schmidt⁸, Verena J. Schuenemann^{3,9}, Ella Reiter^{3,9}, Madita S. Kairies¹⁰, Rainer Weiß¹¹, Susanne Arnold¹¹, Joachim Wahl^{10,11}, Jill A. Hollenbach¹², Oliver Kohlbacher^{5,13,14,15,16}, Alexander Herbig^{1,3}, Paul J. Norman^{6#}, and Johannes Krause^{1,17,3#}

¹ Max Planck Institute for the Science of Human History, Kahlaische Strasse 10, 07745 Jena, Germany

² Institute of Clinical Molecular Biology, Kiel University, Rosalind-Franklin-Strasse 12, 24105 Kiel, Germany

³ Institute of Archaeological Sciences, University of Tübingen, Rümelinstrasse 23, 72070 Tübingen, Germany

⁴ Max Planck Institute for Infection Biology, Charitéplatz 1, 10117 Berlin, Germany

⁵ Applied Bioinformatics, Dept. for Computer Science, University of Tübingen, Sand 14, 72076 Tübingen, Germany

⁶ Division of Biomedical Informatics and Personalized Medicine, and Department of Immunology & Microbiology, University of Colorado, CO 80045, USA

⁷ Immunogenetics Unit, Técnicas Genéticas Aplicadas a la Clínica (TGAC), Mexico City, Mexico

⁸ DKMS, Kressbach 1, 72072 Tübingen, Germany

⁹ Institute of Evolutionary Medicine, University of Zurich, Winterthurerstrasse 190, 8057 Zurich, Switzerland

¹⁰ Institute for Archaeological Sciences, WG Palaeoanthropology, University of Tübingen, Rümelinstrasse 23, 72070 Tübingen, Germany

¹¹ State Office for Cultural Heritage Management, Stuttgart Regional Council, Berliner Strasse 12, 73728 Esslingen, Germany

¹² UCSF Weill Institute for Neurosciences, Department of Neurology, University of California, San Francisco, USA

¹³ Institute for Bioinformatics and Medical Informatics, University of Tübingen, Sand 14, 72076 Tübingen, Germany

¹⁴ Quantitative Biology Center, University of Tübingen, Auf der Morgenstelle 10, 72076 Tübingen, Germany

¹⁵ Translational Bioinformatics, University Hospital Tübingen, Sand 14, 72076 Tübingen, Germany

¹⁶ Biomolecular Interactions, Max Planck Institute for Developmental Biology, Max-Planck-Ring 5, 72076 Tübingen, Germany

¹⁷ Max Planck Institute for Evolutionary Anthropology, Deutscher Platz 6, 04103 Leipzig, Germany

*equal contribution

#corresponding authors

Abstract

Pathogens and associated outbreaks of infectious disease exert selective pressure on human populations, and any changes in allele frequencies that result may be especially evident for genes involved in immunity. In this regard, the 1346-1353 *Yersinia pestis*-caused Black Death pandemic, with continued plague outbreaks spanning several hundred years, is one of the most devastating recorded in human history. To investigate the potential impact of *Y. pestis* on human immunity genes we extracted DNA from 36 plague victims buried in a mass grave in Ellwangen, Germany in the 16th century. We targeted 488 immune-related genes, including *HLA*, using a novel in-solution hybridization capture approach. In comparison with 50 modern native inhabitants of Ellwangen, we find differences in allele frequencies for variants of the innate immunity proteins Ficolin-2 and NLRP14 at sites involved in determining specificity. We also observed that *HLA-DRB1*13* is more than twice as frequent in the modern population, whereas *HLA-B* alleles encoding an isoleucine at position 80 (I-80+), *HLA C*06:02* and *HLA-DPB1* alleles encoding histidine at position 9 are half as frequent in the modern population. Simulations show that natural selection has likely driven these allele frequency changes. Thus, our data suggests that allele frequencies of *HLA* genes involved in innate and adaptive immunity responsible for extracellular and intracellular responses to pathogenic bacteria, such as *Y. pestis*, could have been affected by the historical epidemics that occurred in Europe.

Introduction

Throughout evolution, humans have likely experienced multiple major episodes of infectious disease. Of exceptional virulence and lethality, *Yersinia pestis* has been responsible for at least three major plague pandemics during the last few millennia. Studies of ancient DNA have confirmed *Yersinia pestis* caused widespread infections in Europe from the Late Neolithic period, nearly 5,000 years ago, until the 18th century AD (Andrades Valtuena et al., 2016; Bos et al., 2016; Bos et al., 2011; Feldman et al., 2016; Keller et al., 2019; Namouchi et al., 2018; Rascovan et al., 2019; Rasmussen et al., 2015; Spyrou et al., 2018; Wagner et al., 2014). Historical records show the first pandemic began with the Justinianic Plague in the 6th century AD and lasted until the 8th century, the second began with the 1346-1353 Black Death and continued with thousands of local plague outbreaks until the 18th century (Biraben, 1976; Büntgen, Ginzler, Esper, Tegel, & McMichael, 2012) and the third pandemic started in China in the 19th century AD and spread the pathogen worldwide lasting up until the mid-20th century (Morelli et al., 2010; Politzer & WHO, 1954). Of the three recorded pandemics, the Black Death claimed up to half of the European population during its five-year period (Benedictow, 2004). Although *Y. pestis* is now absent from most of Europe, it still causes sporadic infections among humans in the Americas, Africa and Asia, usually transmitted by fleas from rodent populations that serve as plague reservoirs (Drummond et al., 2014; WHO, 2017). Although the lethality of plague is very high without treatment (WHO, 2017), it remains likely that specific individuals are protected from, or more susceptible to, severe disease through polymorphism in the determinants of natural immunity. In this case, any changes in allele frequencies that occurred during a given epidemic crisis could be evident as genetic adaptation and detectable in modern day individuals.

There are multiple examples of natural selection affecting human immunity-related genes that can be attributed to challenge by pathogens. These examples include specific pathogens causing malaria, cholera or Lassa fever, or to wider differences in pathogen exposure between geographically discrete populations (Harrison et al., 2019; Karlsson et al., 2013; F. M. Key et al., 2014; Kwiatkowski, 2005; McManus et al., 2017; Sabeti et al., 2007; Voight, Kudaravalli, Wen, & Pritchard, 2006; Wang, Kodama, Baldi, & Moyzis, 2006). The toll like receptors (TLRs) are innate immune proteins that detect the presence of specific pathogens to initiate an immune

response. Signatures of purifying selection have been identified within specific *TLR* genes that correlate with distinct pattern specificities of the encoded allotypes (Barreiro et al., 2009). In another example, recent signatures of positive selection in the *IFITM3* gene accompany differential abilities of the alternative variants to control pandemic H1N1 influenza A virus infection (Albright, Orlando, Pavia, Jackson, & Cannon Albright, 2008; Everitt et al., 2012). A final example of human genetic adaptation to pathogens is the 32 base pair deletion in the chemokine receptor *CCR5* (*CCR5-Δ32*), which prevents HIV from entering and infecting human T-cells (Dean et al., 1996). Although once postulated as a plague resistance allele (Stephens et al., 1998), there is little evidence for positive selection acting on *CCR5-Δ32* (Sabeti et al., 2006). By contrast, the Major Histocompatibility Complex (*MHC*), which encodes multiple immunity-related genes including the Human Leukocyte Antigen (*HLA*) molecules, does show evidence for recent positive and balancing selection and has established roles initiating and directing the immune response to infection (Klebanov, 2018; Parham & Moffett, 2013; Prugnolle et al., 2005; Trowsdale & Knight, 2013).

Here, we extracted genomic DNA from 36 individuals who apparently died from plague (*Y. pestis*) in Ellwangen in Southern Germany during the 16th century. We also extracted DNA from 50 modern day Ellwangen inhabitants. We then compared their frequency spectra for a large panel of immunity-related genes. We observed evidence for pathogen-induced changes in allele distributions for two innate pattern-recognition receptors and four *HLA* molecules. We propose that these frequency changes could have resulted from *Y. pestis* plague exposure during the 16th century.

Results

Archaeological and Anthropological Findings

Ellwangen is a small town of 27,000 inhabitants situated in South Germany near the border of Baden-Wuerttemberg and Bavaria. Ellwangen was founded in the 7th century AD, with only a few hundred inhabitants until modern times. The town was affected by multiple plague outbreaks during the 16th and 17th centuries (Ellwangen, 2007). From 2013 to 2015 an excavation took place in Ellwangen during the restoration of the town's market square (Figure 1). Three mass graves were discovered with a total of 101 inhumated remains (Supplementary Figure 1A).

Consistent with 16th century bubonic plague predominantly affecting children (Bowsky, 1971; Clouse, 2002; Cohn, 2003) only 23 of the individuals had reached adult age (Supplementary Note 1). The individuals were buried close to each other and there was little sediment between the distinct layers. The proximity, as well as radiocarbon dating, suggests that all three mass burials were created during the same epidemic crisis event during the 16th century (Supplementary Figure 1B). Genomic DNA from *Y. pestis* was identified previously from 13 of the individuals, and the complete genome of a strain consistent with the era was reconstructed from one of them (Spyrou et al., 2019; Spyrou et al., 2016). We also performed shotgun sequencing directly on DNA libraries prepared from tooth samples of 30 distinct individuals, and pathogen screening using the metagenomic alignment tool MALT (Vågene et al., 2018) identified reads matching to *Y. pestis* in 25 of them, with aDNA characteristic terminal substitutions in samples with sufficient coverage (Supplementary Table 1), confirming that the reads are of ancient DNA origin. With exception of one sequence read of Hepatitis B Virus in one of the petrous bone samples (ELW012), no evidence of other pathogens was detected. Additional archaeological and anthropological findings suggest little physical trauma, albeit poor health condition prior to death, which can likely be considered as normal health and nutrition status for people living in that time period (Supplementary Note 1). Taken together, these findings strongly suggest that these individuals were victims of a single *Y. pestis* plague outbreak that occurred during the 16th century.

The 16th century Ellwangen plague victims display genetic similarity with modern inhabitants

From the 16th century mass grave site in Ellwangen, we successfully extracted DNA from 40 petrous bones (Supplementary Figure 1C) and four teeth. DNA of sufficient quality and quantity for genome wide sequence analysis was obtained from all samples. An average of 1.76 million unique, human genome reads per individual was generated by shotgun sequencing (Supplementary Data 1A). Kinship analysis revealed three pairs of individuals to be first-degree relatives (Supplementary Data 1B, Supplementary Figure 2). In order to obtain the most accurate frequency distributions, one in each pair of the directly related individuals was removed from the allele frequency calculations. In these cases, the individual having the lowest yield of sequence reads was excluded (Material and Methods). In addition, one individual who was second-degree related to two of the other individuals was also excluded (ELW030). We also obtained genomic

DNA samples from 51 contemporary inhabitants of Ellwangen and shotgun-sequenced them with an average of 2.74 million unique human genome reads per individual (Supplementary Data 1A). Here, we identified a single pair of first-degree relatives and removed one individual. In order to test whether the two cohorts derive from a single continuous population, we tested for population genetic similarity using Principle Component Analysis (PCA) (Patterson, Price, & Reich, 2006) and ADMIXTURE analysis (Alexander, Novembre, & Lange, 2009). Showing that the 16th century and modern groups indeed are genetically very similar, we found that the 16th century Ellwangen plague victims form a tight cluster in PCA space, which overlaps with the modern inhabitants (Figure 2A). This finding is bolstered by the highly similar genetic ancestry composition of the two groups as illustrated by their population admixture proportions (Figure 2B). This latter finding is important because recent demographic changes could alter allele frequencies of the modern compared with the 16th century group (Hellenthal et al., 2014).

Two immunity-related genes harbor strongly differentiated SNPs

In order to compare the allele spectra of immunity-related genes in the 16th century *Y. pestis* plague victims with modern-day inhabitants of Ellwangen, we developed an in-solution hybridization capture approach to enrich for 488 human genes implicated in immunity (Supplementary Table 2). This approach allowed us to specifically target the genes of interest while reducing the amount of sequencing required, leading to an average of 308 times more reads on target compared to undirected genome wide sequencing (Supplementary Figure 3). We applied this ‘immunity capture’ method to all 16th century and modern DNA samples. The targeted genes were covered with a mean read depth of 55.8 (Supplementary Data 2). We investigated the allele spectra of the 488 immunity-related genes by leveraging a branching statistic, *Differentiation with Ancestral (Danc)* (F.M. Key, Fu, Romagné, Lachmann, & Andrés, 2016). *Danc* is calculated per site and uses derived allele frequency estimates across three populations; 16th century and modern Ellwangen, and a non-European outgroup (we used Han Chinese from Beijing (Abecasis et al., 2012)). *Danc* scores can range from -1 to +1, and those in the respective far tails of the distribution identify candidates for simulation studies that could indicate positive selection has occurred. We established the expected distribution of *Danc* scores (Supplementary Data 3) under neutrality through simulations using a human demographic model (Gravel et al., 2011).

In our analysis, the distribution of *D_{Anc}* scores closely matches between the simulated and test data (Supplementary Figure 4, Supplementary Table 3). In the far tail of the distribution (>99.9%) we observed three SNPs, two in the Ficolin-2 (FCN2) gene and one in the NOD-like receptor purine domain containing 14 (NLRP14) gene (Table 1) also corresponding to the greatest F_{ST} values among the 488 genes for the same three SNPs (Supplementary Data 4). F_{ST} is an established measure for population differentiation and corrects for expected heterozygosity and sampling error (Weir & Cockerham, 1984). However, due to the ascertainment of SNPs, which are not representative of the whole genome, the far tail of the observed *D_{Anc}* or F_{ST} distribution is no evidence alone for positive selection. Alternatively, we compared the fraction of SNPs observed in the far tail of the simulated and test distribution, which suggest no enrichment of SNPs in our test data and thus no evidence for positive selection using the data at hand (Supplementary Table 3). Further analyses using a larger sample size and whole genome data is necessary in order to understand the role of positive selection due to historic epidemics.

The identified SNPs of FCN2 are a 5' UTR promoter variant [rs17514136 (-4 A to G)] and one coding change variant [rs17549193 (717 C to T; 236 Thr to Met)]. The UTR and coding change variants occur in complete linkage disequilibrium ($\Delta' = 1.0$, $R^2 = 0.9$), and appear to represent a single haplotype that has risen in frequency in the modern population. Interestingly, FCN2 binds to specific molecules on the surface of bacteria, triggering the complement pathway to neutralize the pathogen (Hoang et al., 2011; Luo et al., 2013). The promoter variant is associated with increased serum concentration of FCN2 (Cedzynski et al., 2007), whereas polymorphism at residue 236 (rs17549193) affects binding to the target bacteria (Hummelshoj et al., 2005). Similarly, NLRP14 belongs to inflammasome complex proteins, which are intracellular pattern recognition receptors that trigger local and systemic responses to microbial invasion (Martinon, Burns, & Tschopp, 2002). Inflammasomes are implicated in the immune response to *Yersinia* infection, amongst other pathogens (Philip, Zwack, & Brodsky, 2016; Vladimer, Marty-Roix, Ghosh, Weng, & Lien, 2013). The NLRP14 SNP is a coding change variant (rs10839708 [2745 G to A: 808 Glu-Lys]) that occurs in the leucine-rich repeat (LRR) domain, which in related molecules controls the ligand specificity (Inohara, Chamaillard, McDonald, & Nunez, 2005). Thus, in summary we show immune-related genes have no significant frequency changes

between 16th century *Y. pestis* victims and modern Ellwangen inhabitants.

No evidence for role of CCR5-Δ32 in protection from *Y. pestis* infection

We investigated the Δ32 deletion in the CCR5 locus (chr3:46414947-46414978), which was included in our target regions because this mutation has previously been suggested as protective from the plague. We found that CCR5-Δ32 has a frequency of 16.6% in the 16th century compared to 10.8% in the modern individuals (p=0.27) and 11.2% in Germany (Supplementary Data 5A and 5B, Supplementary Data 6A, Table 2). Consistent with epidemiological modeling and lack of evidence that CCR5 can serve as a *Y. pestis* receptor (Galvani & Slatkin, 2003) this finding suggests that the CCR5-Δ32 mutation provided no protection from *Y. pestis*. Similarly we also investigated SNPs *rs4986790*, *rs4986791* within the gene *TLR4* previously suggested to be associated with resistance to *Y. pestis* (Al Nabhani, Dietrich, Hugot, & Barreau; Laayouni et al., 2014). However, we did not find any significant differences in their respective frequencies (Supplementary Table 4).

Natural selection has increased HLA-DRB*13 and reduced HLA-B*51 and -C*06 frequencies in modern individuals

With more than 28,000 distinct alleles described (Robinson et al., 2015), HLA molecules are encoded by the most polymorphic gene complex in humans. When human populations are exposed to novel diseases through contact with populations or environments they had not encountered previously, changes in *HLA* allele frequencies can occur rapidly (Lindo et al., 2016; Patin et al., 2017). Consequently, the signatures of balancing selection in the genomic region that contains *HLA* are consistently the strongest in the genome (Quintana-Murci, 2019; Sabeti et al., 2006), and specifically correspond to amino acid residues that bind peptide fragments derived from pathogens (Bjorkman & Parham, 1990). Significant shifts in *HLA* allele frequencies can thus reveal evidence of natural selection for specific pathogen resistance. We were able to identify *HLA class I* (-A, -B, -C) and *HLA class II* (-DPA1, -DPB1, -DQA1, -DQB1 and -DRB1) genotypes from all of the 16th century and modern inhabitants of Ellwangen. We observed a total of 86 distinct *HLA class I* alleles, 66 distinct *HLA class II* alleles and 168 distinct *HLA* haplotypes (Supplementary Data 6B). The most frequent haplotype (*HLA-A*01:01~B*08:01~C*07:01~DRB1*03:01*) is the same in both groups and is also the most

common and widespread across Europe today (Darke et al., 1998; Dunne, Crowley, Hagan, Rooney, & Lawlor, 2008; Johansson, Ingman, Mack, Ehrlich, & Gyllensten, 2008; Nowak et al., 2008; Pingel et al., 2013). Thus the diversity and composition of *HLA* haplotypes appears as expected for Northern European populations (Alfirevic et al., 2012), and we did not observe any significant differences in their frequencies between the 16th century and modern individuals.

By contrast to the haplotype distributions, on examining the individual *HLA class I* genes, we observed that the *B*51:01* allele of *HLA-B* decreased from 15.3% in the 16th century Ellwangen plague victims to only 6.0% ($p=0.04$ (p -corrected = NS); $DANc = -0.093$) in the modern Ellwangen population (Table 3, Supplementary Data 4, Supplementary Data 5A). Similarly, the *C*06:02* allele of *HLA-C* decreased from 13.9% to 5% ($p=0.04$ (p -corrected = NS); $DANc = 0.053$). *HLA-B*51:01* and *-C*06:02* are not in linkage disequilibrium in either population (Supplementary Data 6B), and so these two observations are independent. In addition, although there were no significant frequency differences observed for any *HLA class II* alleles as determined at two-field resolution, we observed that all allotypes present representing the DR13 serological group (Holdsworth et al., 2009) were at substantially lower frequency in the 16th century than modern Ellwangen population. Accordingly, by considering them together, there was an increase in *DR13* frequency from 5.6% in the 16th century to 17.0% in the modern individuals ($p=0.026$, Table 3, Supplementary Data 5A). Repeating this analysis for all the major DRB1 lineages present (Holdsworth et al., 2009), showed DRB1*13 as the only allotype differing in frequency between the two groups (Table 3). We used Wilson Score Interval estimation of the 95% binomial confidence interval. The 95% CI of *HLA-B*51:01* was 0.09 – 0.25 (observed = 0.06), the 95% CI of *HLA-C*06:02* was 0.08 – 0.24 (observed = 0.05), and DRB1*13 was 0.02 – 0.13 (observed = 0.16). Thus, for each of the three *HLA* allotypes showing distinctions between modern and 16th century inhabitants of Ellwangen, the observed modern allele frequencies are outside the 95% binomial confidence intervals surrounding sampling of the 16th century allele frequencies. We further validated these findings by comparing the *HLA* allele frequencies observed in the Ellwangen individuals with a large panel ($N=8,862$) of unrelated bone marrow donor registry volunteers gathered from all of Germany (Supplementary Data 5B). Whereas there were no significant allele frequency differences when comparing modern inhabitants of Ellwangen with modern Germany as a whole, we observed significantly lower

frequencies of *B*51:01* in modern Germany (5.5%) than the Ellwangen plague victims (15.3%), when applying a pairwise proportion test ($p=0.005$; $DANc=-0.098$). We also observed differences in *HLA-C*06* and *DRB1*13* between the plague victims and modern Germany, but these were not statistically significant (Supplementary Data 5B).

To distinguish if the changes in frequencies of *B*51:01*, *C*06:02* and *DRB1*13:01* were more likely to be due either to natural selection or genetic drift we performed forward time simulations by starting from the observed polymorphisms in the 16th century Ellwangen and modelling neutrality for the last 500 years. This way it was possible to start from reasonable levels of genetic variation without the necessity to determine the impact of ancient selection on HLA and episodic turnover of HLA alleles. Moreover, this way each allotype could be tested individually. Again, we observed an overall concordance between median frequencies of the simulated neutral alleles and the modern Ellwangen allele frequencies, as is expected under genetic drift. By contrast, the allele frequencies of *B*51:01*, *C*06:02* and *DRB1*13:01* observed for modern inhabitants of Ellwangen were in the extreme tails of their respective distributions ($p^{sim}=0.006$, 0.004 , <0.001 , respectively, Figure 3), suggesting natural selection likely drove the change in these allele frequencies. A similar significant shift was observed when we considered DR13 broadly ($p^{sim}<0.001$). To quantify the selection coefficient (s) responsible for these changes, we performed the simulations incorporating selection, mirroring the timeline of the plague, across a range of s values. We identified an s equal to -0.25 was most likely to produce the observed decrease in *B*51:01* alleles as well as an s equal to -0.27 in case of *C*06:02*. An s of 0.37 was most likely to cause the increase in *DRB1*13:01* (Supplementary Figure 5). Notably, these values are within the range of previously reported values of s acting on MHC (Radwan, Babik, Kaufman, Lenz, & Winternitz, 2020).

Higher incidence of KIR3DL1 interaction with HLA-B in plague victims than modern inhabitants of Ellwangen

The binding specificity of HLA allotypes, and thus their function and distinctiveness, is determined by specific amino acid residues in the alpha-helix of the molecule. Polymorphism of these amino acid residues is associated with autoimmune diseases and response to pathogens (Achkar et al., 2012; Hammer et al., 2015; Hollenbach et al., 2019; Sun et al., 2018). We

identified three of these residues having significant ($p < 0.05$) differences in frequency between the 16th century victims and modern individuals (Supplementary Data 7A). We observed histidine (H) at position 9 of HLA-DPB1 to be approximately three times more frequent in the 16th century (13%) than the modern (4%) individuals ($p = 0.03$ (p -corrected = NS); $DANc = 0.13$); Supplementary Data 7A). We also observed isoleucine (I) at position 80 (I-80) in HLA-B twice as frequently in the 16th century (28%) than in the modern individuals (15%) ($p = 0.04$ (p -corrected = NS); $DANc = 0.28$), and aspartic acid (D) at position 114 in HLA-C more frequently in the 16th century (85%) than the modern (70%) individuals ($p = 0.02$ (p -corrected = NS); $DANc = -0.062$); Supplementary Data 7A). Residue D-114 is located in the outward-facing groove of HLA-C and its variation can directly affect the sequence of endogenous peptides able to bind (Di Marco et al., 2017). Since *HLA-B* alleles encoding I-80 are most commonly observed on haplotypes that also have *HLA-C* alleles that encode D-114 (Cao et al., 2001), it is likely that the observed frequency difference at this position is driven by linkage disequilibrium with *HLA-B*. *HLA-B**27:02, -B*38:01, -B*49:01, -B*51:01, -B*52:01, -B*57:01 and -B*58:01 are all I-80⁺ allotypes that are more frequent in the 16th century than the modern inhabitants of Ellwangen (Supplementary Data 7B and 7C), together accounting for the observed difference in I-80 frequency (Table 3). Thus, it is likely that the significant difference in frequencies we observed for *HLA-B**51:01 can be attributed to the fact that it possesses an isoleucine at position 80. We next tested whether the observed frequency changes in *HLA-DPB1* H-9 and *HLA-B* I-80 were more likely due to genetic drift or natural selection, using neutral forward genetic simulations as above. In both cases, we found these allele frequency shifts were unlikely to be observed unless natural selection was included in the model (*HLA-DPB1* H-9 $p^{sim} = 0.014$, *HLA-B* I-80 $p^{sim} = 0.002$).

KIR genes encode surface proteins on natural killer (NK) cells whose interaction with HLA class I molecules can determine the outcome of NK cell responses (Guethlein, Norman, Hilton, & Parham, 2015). For example, polymorphism of residue 80 in *HLA-B* controls its ability to bind to KIR3DL1, with I-80 defining ligand specificity and permitting the strongest interaction (Saunders et al., 2015). We therefore sought to determine whether the observed high frequency of *HLA-B* I-80⁺ alleles in the 16th century samples affects the frequency of *HLA-B* interaction with KIR3DL1. The *KIR* region varies by gene content (Uhrberg et al., 1997), and we were able

to determine this diversity across all the 16th century individuals (Supplementary Figure 6). We observed that 97% of the 16th century individuals possess at least one copy of *KIR3DL1*, compared to 88% of the modern Ellwangen samples. These values are within the range observed in modern European populations (Hollenbach, Nokedal, Ladner, Single, & Trachtenberg, 2012) as well as those predicted in our neutral forward genetic simulations ($p^{sim}=0.258$). Thus, we observe no statistically significant differences in *KIR3DL1* gene frequencies between the 16th century and modern samples (Table 4A). Similarly, we observed no difference in *KIR3DL1* allele frequencies (Supplementary Data 6C) between the 16th century and modern individuals (Table 4A). By contrast, we found that *KIR3DL1* and *HLA-B I-80*⁺, and thus their combined genotype, is more frequent in 16th century (53%) than modern (26%) individuals ($p=0.011$ (p-corrected = NS), Table 4B). Using simulations, we found that genetic drift was unlikely to produce the modern day observed frequencies of *HLA-B I-80* and *KIR3DL1*, but that selection against *HLA-B I-80* likely drove the decreased *HLA-B I-80*⁺/*KIR3DL1*⁺ joint genotype frequencies ($p^{sim}=0.002$).

Discussion

In this study we investigate a large panel of immunity-related genes from 36 individuals discovered in three 16th century plague mass graves in Ellwangen, Southern Germany, and compare them to 50 present-day inhabitants of Ellwangen. For this purpose, we developed a targeted DNA capture protocol comprising 488 human immune system genes including the six major *HLA class I* and *class II* genes and the *KIR* locus. We also compared the 16th century *HLA* allele frequencies with sequence data of 8,862 potential stem cell donors registered with DKMS (German Bone Marrow Donor Registry). Although we observe a predominant genetic stability of human immune genes over at least five centuries in Central Europe, we find distinct allele frequency changes in the *HLA* and in two other genes that encode components of innate immunity.

Given its devastating effect, the *Y. pestis*-driven 2nd plague pandemic is a strong candidate for exerting selection pressure on the human immune response (Laayouni et al., 2014; Lenski, 1988). We observed strong allele frequency differences at SNPs located in the *FCN2* and *NLRP14* genes, albeit we find no clear evidence that positive selection has contributed to the

observed allele frequency differentiation. Both of these molecules are pattern recognition receptors that bind specific pathogen-derived components to initiate the inflammation response; Ficolin-2 does this extracellularly, and NLRP14 intracellularly. Ficolin-2 promotes phagocytosis of pathogenic bacteria (Hoang et al., 2011; Luo et al., 2013). Interestingly, we observed two SNPs of known direct functional effect to be in strong LD, forming a single haplotype that is elevated in frequency in the modern compared to the 16th century individuals. This haplotype both increases serum concentration and alters the binding properties of Ficolin-2 (Cedzynski et al., 2007; Hummelshoj et al., 2005), which makes it a good candidate for providing improved resistance to *Y. pestis* infection. On the other hand, less is known about NLRP14, which has similar domain organization to other inflammasome proteins. Inflammasomes act to trigger inflammation as well as self-destruction of infected cells (Lamkanfi & Dixit, 2014) and have been identified recently as important mediators of the immune response to *Y. pestis* (Park et al., 2020). Interestingly, the same variant we observed at lower frequency in modern individuals than plague victims (K-808) was identified at high frequency due to positive selection in the Human Genome Diversity-Project populations from East-Asia (Vasseur et al., 2012). Similar inflammasome molecules, including NLRP3 and NLRP12, are known to respond to *Y. pestis* (Vladimer et al., 2013; Vladimer et al., 2012), but may also be exploited by bacteria to inhibit immunity (Anand et al., 2012; Philip et al., 2016; Zaki, Man, Vogel, Lamkanfi, & Kanneganti, 2014). K-808 is located in the LRR domain of NLRP14 and influences ligand specificity. Therefore, the fluctuating frequencies of the variants at this position point to an evolutionary battle between host and pathogen (Abi-Rached, Dorigi, Norman, Yawata, & Parham, 2007). Functional tests are thus required to determine if mutation at residue 808 permits recognition of any components of *Y. pestis*.

On examination of *HLA* alleles we observed candidates for natural selection of human adaptive immune responses. HLA class I and II are cell surface molecules that bind to peptides derived from intracellular or extracellular proteins, respectively. To trigger and drive the adaptive immune response, these peptides are presented by the HLA molecules to T-cells. Antibody production is elicited through highly polymorphic HLA class II molecules, HLA-DP, -DQ, and -DR, presenting pathogen-derived peptides to CD4⁺ T-cells (Neefjes, Jongma, Paul, & Bakke, 2011). Direct killing of infected cells can occur when any of three highly polymorphic HLA class I molecules, HLA-A, -B or -C, presents pathogen-derived peptides to cytotoxic CD8⁺ T-

cells (Doherty & Zinkernagel, 1975). The *HLA-DRB1*13* allelic group increased in frequency from 5.6% in the plague victims to 17% in the modern Ellwangen individuals and 12% in the German bone marrow donors, potentially indicating antibody-driven protection from the plague for individuals having this allotype. *HLA-DRB1*13* is associated with resistance to *M. tuberculosis* (Dubaniewicz, Lewko, Moszkowska, Zamorska, & Stepinski, 2000). Similar to *Y. pestis*, *M. tuberculosis* can invade and survive within macrophages (Pieters, 2008). Macrophages express high levels of HLA class II and are cells that are specialized for presenting peptides to CD4+ T cells to initiate antibody production. These HLA class II molecules can present antigens from intracellular pathogens, such as *M. tuberculosis* (Ankley, Thomas, & Olive, 2020). Thus, the same adaptive immune pathway triggered by *HLA-DRB1*13* that provides resistance to *M. tuberculosis*, might also provide resistance to *Y. pestis*.

Some HLA class I allotypes interact with killer-cell immunoglobulin-like receptors (KIRs) to modulate the function of Natural Killer (NK) cells, which are essential components of innate immunity, providing front-line defense against infection (Guethlein et al., 2015; Long, Kim, Liu, Peterson, & Rajagopalan, 2013). The *KIR* locus varies by gene content (Uhrberg et al., 1997; Wilson et al., 2000) and is located on a separate chromosome (chr19) to HLA (chr6). Combinatorial diversity of HLA class I and KIR allotypes directly impacts NK cell responses to infection (Bashirova, Martin, McVicar, & Carrington, 2006; Parham & Moffett, 2013). We observed a lower frequency of the HLA-B allotypes that can interact with KIR3DL1 in the modern individuals than we did in the plague victims, suggesting this combination could have been disadvantageous for individuals infected with *Y. pestis*. KIR3DL1 is an inhibitory receptor that enables NK cells to respond strongly to changes in HLA expression by infected cells (Boudreau & Hsu, 2018; Saunders et al., 2015) (Gumperz, Litwin, Phillips, Lanier, & Parham, 1995). Finally, we observed a marked decrease in the frequency of *HLA-C*06:02* when comparing the 16th century and modern Ellwangen populations. *HLA-C*06:02*, which also interacts strongly with KIR (Hilton et al., 2015), is strongly associated with psoriasis (Ogawa & Okada, 2020), an immune-mediated disease. These observations implicate excess collateral damage caused by NK cells responding to infection (Guo, Patil, Luan, Bohannon, & Sherwood, 2018; Kim et al., 2008), as a potential mechanism of pathology.

A limitation of this study is the relatively small sample size of 36 plague victims from the 16th century. As suggested by our effect size analyses (Supplementary Figure 7), with the given sample size only large effects ($w = 0.40 - 0.45$) can be detected, and therefore, the observed frequency changes do not withstand multiple testing correction. Thus, it also remains possible that the signals of selection we detected for some variants are caused by drift and/or sampling biases, and, on the other hand, some other variants under selection were potentially not targeted through this approach. Increasing the sample size in future studies will allow addressing this caveat. Moreover, all tested individuals are 16th century late plague victims, and it remains possible that stronger selection signatures could be observed when analyzing individuals who died of plague in earlier pandemics. Importantly, further cohorts of *Y. pestis* victims are required to verify the observations in this study in different geographic contexts, and also whether the associations with the above-mentioned immunity genes are specific to the plague or might be caused by other pathogens (Galvani & Slatkin, 2003). Furthermore, the demographic model we used for simulation of natural selection is fitted to the CEU population (Central Europeans from Utah) (Gravel et al., 2011) and assumes an exponential population growth. However, the CEU population might have had a different demographic history than Ellwangen. It cannot, therefore, be ruled out that the results from our analysis of natural selection may be inaccurate, if Ellwangen has undergone stronger genetic drift than CEU. Nevertheless, our simulation results provide preliminary evidence for natural selection as the main driving agent for the decrease of frequencies in HLA-C*06:02, HLA-B*51:01 (and other HLA-B I-80⁺ alleles), and HLA-DPB1-H9 on the one hand, and the frequency-increase in HLA-DRB1*13 on the other hand. We note that the frequency changes we observed are based on simulations of episodic selection and could also be derived through alternative scenarios, including constant selection pressure (e.g. s of -0.012 B*51, -0.014 C*06, 0.06 DRB1*13); (data not shown), or other epidemic challenges, such as smallpox or tuberculosis, occurring since the 16th century. However, we did not find evidence of smallpox or tuberculosis in the plague victims' DNA. Comparison with non-plague victims from the same time period will be necessary to definitively answer this question. Our results do not provide support for the proposition that evolution of human immunity drove reduction of *Y. pestis* virulence and its disappearance from Europe (Ell, 1984). Instead, we provide first evidence for evolutionary adaptive processes that might be driven by *Y. pestis* and may have been shaping certain human immunity-relevant genes in Ellwangen and possibly also in Europe. As the earliest

victims of *Y. pestis* in Europe were already present in the Late Neolithic (Andrades Valtuena et al., 2016; Rascovan et al., 2019; Rasmussen et al., 2015) and Europeans were intermittently exposed to plague for almost 5,000 years, it is possible that relevant immunity alleles had already been pre-selected in the European population long ago and maintained by standing variation (Ralph & Coop, 2015) but recently became selected through epidemic events. Whilst *Y. pestis* seems a likely culprit, this remains to be determined through replication cohorts and further functional analyses.

Material and Methods

Anthropological analyses

Anthropological analyses on the skeletal remains were conducted in the Institute of Paleoanthropology, University of Tübingen. Diseases of the periodontium and the teeth, nonspecific stress markers and deficiencies, degenerative transformations, inflammatory bone changes, and trauma were recorded (Supplementary Note 1). The body height of the adult individuals was reconstructed and the growth course of the sub adult individuals was analyzed (Kairies, 2015).

C14-Dating of the archaeological remains from Ellwangen

Acceleration Mass Spectrometry Radiocarbon (AMS-C14) dating was conducted at the Curt-Engelhorn Center for Archaeometry in Mannheim. Calibration was performed based on the INTCAL13 and the SwissCal 1.0 calibration curves.

DNA extraction

Petrous pyramids were cut longitudinally in order to enable access to the bony labyrinth (Supplementary Figure 1C), which is the densest part of the mammalian body (Frisch, Sorensen, Overgaard, Lind, & Bretlau, 1998) and provides the highest endogenous DNA yields (Pinhasi et

al., 2015). After cleaning the surface on one side of the bony labyrinth with the drill bit, sampling was performed along the semicircular canal, which yielded 80-120 mg bone powder. DNA extraction was performed by guanidinium-silica based extraction (Rohland & Hofreiter, 2007) using all the bone powder obtained. Tooth samples were cut in the middle, thus separating the crown from the root, followed by drilling into the dental pulp to produce bone powder (ca. 100 mg). Saliva samples were obtained from 51 living Ellwangen citizens using *Whatman OmniSwab* cheek swabs. Samples were obtained only from individuals whose families have been resident in Ellwangen for at least four generations. Consent was given by the contributing persons and their samples were anonymized. Approval for the study was granted by the Ethics Committee of the Faculty of Medicine of the Eberhard Karls University and the University Hospital Tübingen. Isolation of genomic DNA was performed using the *QIAamp DNA Blood Mini Kit* following the *Qiagen* protocol.

Preparation of libraries and sequencing

Overall strategy: Indexed libraries were generated from all samples and the sequencing was then performed in two stages. First, an aliquot of the full DNA library was subjected to whole genome sequencing. Then, a second aliquot was subjected to enrichment for selected immunity-related genes and subsequently sequenced.

Since our protocols for DNA extraction and library preparation are optimized for short-length ancient DNA, and in order to avoid potential bias through laboratory methods, we sheared the DNA extracted from modern individuals using ultrasonic DNA shearing to the same average length as the ancient DNA. Therefore, the modern DNA was sheared to an average fragment length of 75 bp using a *Covaris M220 Focused ultrasonicator*. DNA libraries, including sample-specific indices, were prepared using 20 µl of each extract following published protocols (Kircher, Sawyer, & Meyer, 2012; Meyer & Kircher, 2010). For the ancient samples, partial uracil-DNA-glycosylase treatment was first applied (Rohland, Harney, Mallick, Nordenfelt, & Reich, 2015). Sequencing was performed using an *Illumina HiSeq 4000* instrument with 75+8 cycles in single-end mode.

Screening for pathogens

DNA samples were screened for their metagenome content using the alignment tool MALT version 0.3.8 (Vågene et al., 2018) and the metagenome analyzer MEGAN V6.11.4 (Huson, Auch, Qi, & Schuster, 2007) (Supplementary Table 1).

Since petrous bone samples are not ideal for pathogen screening, we additionally accessed well-preserved tooth samples from 30 distinct 16th century plague victims. Teeth were not available from all individuals from whom we had obtained petrous bones, nor could they be unambiguously attributed to specific individuals. Sequencing libraries and shotgun sequencing were performed on the teeth following published protocols as described above.

MALT was used to align all pre-processed reads against a collection of all complete bacterial genomes obtained from NCBI (<ftp.ncbi.nlm.nih.gov/genomes/refseq/bacteria>, access 12.03.2018). MALT was executed in BLASTN mode for bacteria using the following command: `malt-run --mode BlastN --e 0.001 --id 95 --alignmentType SemiGlobal --index $REF --inFile $IN --output $OUT` (where \$REF is the MALT index). The e-value (--e) is a parameter that describes the number of hits that are expected to be found just by chance. The --id parameter describes the minimum percent identity that is needed for a hit to be reported. As the screening with MALT was performed on aDNA data the applied filters are not very stringent since we expect substitutions in organisms from ancient samples.

Reads assigned to the *Yersinia pestis* node and reads assigned to the nodes below, were extracted using the extract reads function in MEGAN. For subsequent verification blastn (version 2.7.1) was used to blast the extracted reads against *Yersinia pestis* (NC_003143.1) and *Yersinia pseudotuberculosis* (NC_010634.1). The following custom blast command was used:

`blastn -db $REF -query $IN -outfmt "6 qseqid sseqid pident length mismatch gapopen qstart qend sstart send eval bitscore gaps"` (where \$REF is the reference genome and \$IN are the extracted reads from MEGAN).

Targeted sequencing of immunity-related genes

Indexed libraries containing 20 µl DNA each were amplified in 100 µl reactions in a variable number of one to seven cycles to reach the required concentration of 200 ng/µl for enrichment, followed by purification using *Qiagen MinElute* columns. Using an in-solution capture-by-

hybridization approach (Fu et al., 2013), DNA molecule fragments originating from immunity genes were enriched from the total DNA. The design and manufacture of the capture probes are described below. Sequencing was performed as above.

DNA damage estimation

We performed an initial analysis of the merged data using the *EAGER* pipeline (Peltzer et al., 2016) as follows: reads were mapped to *hg19* (The Genome Sequencing Consortium, 2001) using the *aln* algorithm in *BWA 0.7.12* (H. Li & Durbin, 2010) with a seed length (k) of 32, the *samtools* mapping quality parameter “q” set to 30 and a reduced mapping stringency parameter “-n 0.01” to account for damage in ancient DNA. On average 2.2 million reads (51%) from the plague victims with an average length of 59 bp, and 4.2 million reads (91%) from the modern individuals with an average length of 68 bp, mapped uniquely to hg19 (Supplementary Data 1A). To assess the authenticity of the ancient DNA fragments, C to T misincorporation frequencies (Briggs et al., 2007) were obtained using *mapDamage 2.0* (Jonsson, Ginolhac, Schubert, Johnson, & Orlando, 2013). As expected from partial UDG-treatment (Rohland et al., 2015), ancient DNA sequences showed C to T substitutions at the first two positions of their 5’ ends and G to A substitutions at the 3’ ends (Supplementary Data 1A). The first two positions from the 5’ end of the fastq-reads were trimmed off. The modern sample DNA sequence reads were not subjected to this trimming.

Sex determination

Genetic sex was determined based on the ratio of sequences aligning to the X and Y chromosomes compared to the autosomes (Skoglund, Storå, Götherström, & Jakobsson, 2013).

Final data collation

Contamination was estimated through examination of mitochondria sequences using the software *Schmutzi* (Renaud, Slon, Duggan, & Kelso, 2015), and in males additionally on the X-chromosomal level by applying *ANGSD* (Korneliussen, Albrechtsen, & Nielsen, 2014). Contamination estimates ranged between 1 and 3% on mitochondrial and between 0.2 and 2.9% on X-chromosomal level (Supplementary Data 1A). Datasets showing >8% contamination were excluded from further analyses.

Genotyping

SNPs were drawn at random at each position from a previously published dataset of 1,233,013 SNPs (Haak et al., 2015; Lazaridis et al., 2014; Mathieson et al., 2015) in a pseudo-haploid manner using *pileupcaller* from the *sequenceTools* package (Lamnidis et al., 2018). Samples having fewer than 10,000 calls from a set of 1,233,013 SNPs were excluded. Forty-four datasets from ancient samples (40 from petrous bones and four from teeth) and 52 datasets from modern saliva samples remained.

Population genetic analyses

The genotype data from both Ellwangen populations were merged with a dataset of previously published West Eurasian populations genotyped on the aforementioned 1,233,013 SNPs (Mathieson et al., 2015) using the program *mergeit* from the *EIGENSOFT* package (Patterson et al., 2006). Principle Component Analysis (PCA) was performed using the software *smartpca* (Patterson et al., 2006). Admixture modelling was performed using the software ADMIXTURE (Alexander et al., 2009) with 65 West Eurasian populations from the *Affymetrix Human Origin* dataset, and the number of ancestral components ranging from K=3 to K=12. Cross-validation was performed for every admixture model and the model with the highest accuracy was determined by the lowest cross-validation error.

Kinship analysis

Kinship was assessed using three different software packages: *READ* (Monroy, Jose, Jakobsson, & Günther, 2017), *lcMLkin* (Lipatov, Sanjeev, Patro, & Veeramah, 2015) and *outgroup f3* statistics (Patterson et al., 2012). *READ* identifies relatives based on the proportion of non-matching alleles. *lcMLkin* infers individual kinship from calculated genotype likelihoods, and *f3* statistics can be used to identify relatives based on the amount of shared genetic drift. A pair of individuals was regarded related if evidence of relatedness was independently provided by at least two programs. For the modern population a first-degree relationship (parent-child or siblings) was detected by all three programs for EL1 and EL57. For the plague victims, evidence of a first-degree kinship was provided from all three programs for three pairs of individuals: ELW015 and ELW037, ELW016 and ELW017, and ELW036 and ELW039. Support from at

least two programs was given for second degree relatedness (grandparent-grandchild, uncle-nephew or first cousins) for two pairs: ELW021 and ELW030, and ELW007 and ELW039. Second- or higher-degree relatedness was suggested for the pair ELW030 and ELW034. Nine further observations of second-degree relationships were observed, but supported by only one program at a time and therefore not regarded as reliable kinship estimates (Supplementary Figure 2). Individuals EL57, ELW017, ELW030, ELW037 and ELW039 were excluded from allele frequency calculations, since they constitute kinship “nodes” or “leaves” that would bias allele frequencies as they do not contribute to the total allele diversity.

Effect size analysis

Effect sizes were estimated and plotted in *G*Power* 3.1.9.2 (Faul, Erdfelder, Lang, & Buchner, 2007) based on the given sample size and a power of 0.8. Effect size analysis has shown that with the current sample size large to medium effects ($w=0.45-0.4$) could be detected (Supplementary Figure 7).

Probe design for immune-capture

Enrichment of selected target genomic regions prior to sequencing can save sequencing costs and significantly reduce microbial DNA contaminants (Fu et al., 2016; Gnirke et al., 2009; Haak et al., 2015; Lazaridis et al., 2014; Mathieson et al., 2015). We therefore selected a set of 488 different human genes representative of the innate and adaptive immune system (Supplementary Table 2). Exon sequences were extracted from the human genome build *hg19* (The Genome Sequencing Consortium, 2001) using the *RefSeqGene* records from the *NCBI/Nucleotide* database and then selecting “Highlight Sequence Features” and “Exon”. We added alternative alleles for *HLA*, *MIC*, *TAP* and *KIR*, which were obtained from the IMGT/HLA database (Robinson et al., 2015). For *HLA class I* and *KIR* genes the intronic regions were also included. For the *HLA* and *MIC* genes a set of 83 representative alleles with full-length gene sequences was chosen that encompasses the major serologically defined subclasses (Holdsworth et al., 2009) and covers 95% of the known polymorphism. To capture the remaining 5%, a set of 162 x 160 bp consensus sequences was designed.

A 60 bp probe was designed at every 5 bp interval along the target sequence. The last (3') 8 bp of each generated sequence was replaced by a custom primer sequence, so that probes could be

amplified. The final 52 bp probe sequences were mapped to *hg19* using *RazerS3* (Weese, Holtgrewe, & Reinert, 2012) with minimum threshold of 95% identity. Duplicates and probe sequences that mapped more than 20 times were removed. This process resulted in a final set of 322,667 unique probe sequences of 52 bp length. The probe set was tripled to complete capacity of the *Agilent* 1-million feature array. The probes were cleaved from the array and amplified using PCR (Fu et al., 2016). In summary, we generated 322,667 unique probes of 52 bp length using stepwise 5 bp tiling to cover a total of 3,355,736 bp. The final set of probe sequences is available in Supplementary Data 8. To validate the capture protocol, we used seven cell lines from the Immunogenetics and Histocompatibility Workshop (IHW) chosen to represent divergent HLA alleles that we had previously sequenced to full resolution (P. J. Norman et al., 2017). The results are shown in Supplementary Data 2.

Analysis of the CCR5-Δ32 frequency

The CCR5 locus (chr3:46414947-46414978) was included in the target regions. To genotype CCR5 for wildtype (wt) and Δ32 alleles, the sequence data was remapped to *hg19* using *BWA-mem* with the mapping quality filter turned off. To generate genotypes, the CCR5 locus was visually inspected using the Integrative Genomics Viewer (Robinson et al., 2011).

1000 Genome data for selection scan

We obtained the “low coverage” and “exome” aligned data for a set of 50 unrelated individuals for the East Asian population CHB (Han Chinese in Beijing, China) from the 1000 Genomes Phase 3 dataset (<ftp://ftp.1000genomes.ebi.ac.uk/vol1/ftp/phase3/data/>). The bam files were converted into *fastq* format using the *bamtofastq* option from the software *bedtools* 2.28.0 (Quinlan, 2014).

Variant detection

We used *samtools mpileup* (Heng Li et al., 2009) for variant detection with a minimum mapping and base quality of 30 while ignoring indels (-q 30 -Q 30 -C 50 -t DP,SP -g --skip-indels), and used *bcftools* (Heng Li, 2011) for variant calling (-m -f GQ -O b). We considered only variants that were within the captured regions +/- 1,000 bp. Variants were kept when at least 10 individuals had a genotype quality of 30 or higher as measured using *vcftools* (Danecek et al.,

2011). Resulting vcf-files were further annotated by adding the ancestral allele and dbSNP IDs version 147. The ancestral allele was called as the most parsimonious based on 1000 Genomes data (Abecasis et al., 2012) and a multiple species alignment (F.M. Key et al., 2016).

DAnc calculation

For all variants shared across the Ellwangen data (modern and ancient) and 1000 Genomes CHB population we calculated a *Differentiation with Ancestral (DAnc)* score (F.M. Key et al., 2016). *DAnc* is calculated per site, and uses derived allele frequency estimates to infer population-specific allele frequency changes. Therefore, we inferred the derived allele frequency (DAF) using the annotated ancestral allele for every site. Using the DAF we calculated *DAnc* scores per site:

$$DAnc = |(ELW_{MOD} - CHB)| - |(ELW_{ANC} - CHB)|$$

For every site the resulting *DAnc* scores can range from -1 to +1. Invariable sites have a score of 0. A positive *DAnc* score indicates that the modern Ellwangen population has a different allele frequency compared to the ancient Ellwangen population and the outgroup population, e.g. due to recent positive selection. A negative *DAnc* score indicates that the ancient Ellwangen population differentiates from both modern Ellwangen and the outgroup CHB.

Estimating F_{ST} values

We calculated F_{ST} values for all variants using the (Weir & Cockerham, 1984) estimator implemented in *vcf-tools* (Danecek et al., 2011). We report the empirical p-values, which were obtained by comparing the F_{ST} of all three candidate SNPs to the empirical distribution of F_{ST} scores from all other variants.

Simulation of neutral evolution

In order to estimate the expected distribution of *DAnc* scores under neutral evolution, we simulated the European demographic history, using a published model (Gravel et al., 2011) and the simulation software *slim2* (Haller & Messer, 2017). The demographic model is based on genome-wide data; we however had predominantly capture data from coding regions. To account

for increased drift in coding regions due to background selection, we reduced the effective population sizes using background selection coefficients (*B scores*) (F.M. Key et al., 2016). We estimated background selection for every genomic region captured using a published genome-wide map (McVicker, Gordon, Davis, & Green, 2009). The complete model including all parameters is available in Supplementary Data 9. We ran 100,000 simulations of genomic loci matched in length to the captured region and used the resulting variants to calculate the neutral expectation of the *D_{Anc}* score distribution.

Simulation of natural selection

We performed 10,000 forward genetic simulations using *slim3* (Haller & Messer, 2019) to determine null distributions for neutral frequency changes over 500 years in Ellwangen for each HLA and KIR allotype. We used the sampled ancestral Ellwangen HLA and KIR allotype frequencies as input and simulated 20 generations, assuming a 25 year generation time (e.g. Gravel et al, 2011). We assumed a constant population growth rate of 1.085 per generation, resulting in growth from 5000 to approximately 25000 in Ellwangen. We explicitly modelled HLA and KIR allotypes, using linked binary identifiers to differentiate between alleles of a gene, and therefore assumed no new mutations or intragenic recombination. We calculated intergenic recombination rates per generation between *HLA* genes using a recent sex-averaged refined genetic map (Bhérier, Campbell, & Auton, 2017). We allowed free recombination between *HLA* and *KIR* regions (because they are on separate chromosomes). Specifically, we assumed the following number of crossovers per generation between each HLA gene. HLA-A/HLA-C: $5.3e^{-3}$, HLA-C/HLA-B: $1e^{-8}$, HLA-B/HLA-DRB345: $5.4e^{-3}$, HLA-DRB345/HLA-DRB1: $1e^{-8}$, HLA-DRB1/HLA-DQA1: $3.2e^{-5}$, HLA-DQA1/HLA-DQB1: $3.9e^{-7}$, HLA-DQB1/HLA-DPA1: $6.5e^{-3}$, and HLA-DPA1/HLA-DPB1: $1e^{-8}$. We calculated neutral frequency changes of each allotype. We conclude the frequency changes of an allotype is due to natural selection if the sampled modern day allotype frequency falls within the 0.5% extremes of the respective neutral distribution ($p < 0.01$).

We re-implemented the neutral *slim3* models as described above, but included a non-zero *s* parameter for each HLA-allotype in question. For each selected allotype, we ran 100 simulations with a positive or negative *s* with an absolute value of 0.001, 0.01, 0.1, 0.2, 0.3, 0.4, 0.5, 0.6 or 0.7. Mirroring the timeline of the European plague outbreak, allotypes were selected for 7

generations and then returned to neutrality. The reported s values were consistent with previous reported values of s acting on *MHC* genes (Radwan et al., 2020). We estimated the strength of natural selection by fitting a LOESS curve to the simulated relationship between s and allotype frequency and mapping the observed modern Ellwangen allotype frequency.

HLA typing of the Ellwangen individuals

We applied the *OptiType* algorithm, which is a program that enables HLA genotyping from high-throughput sequence data. *OptiType* requires a minimum of a 12-fold coverage to reliably determine the HLA alleles present at two-field (distinct polypeptide sequences) resolution. We applied *OptiType* (Szolek et al., 2014) to identify HLA class I alleles, using a reference set of present-day HLA allele sequences and a required sequence identity of at least 97% for every alignment. We set no limit on the number of potential best matches during read mapping. We manually verified the results obtained by a development version of the upcoming *OptiType* 2.0 package in order to determine HLA class II alleles. For every sample, the *OptiType* call having highest confidence was used.

Reconstruction of HLA haplotypes

Haplotypes were assigned based on previously reported frequencies and linkage disequilibrium (LD) (Cao et al., 2001; González-Neira et al., 2004). Maximum-likelihood haplotype frequencies for alleles and two-point, three-point and four-point associations were estimated using an Expectation-Maximization (EM) algorithm provided by the computer program *Arlequin* ver. 3.5 (Excoffier & Lischer, 2010).

Comparing allele and haplotype frequencies

HLA allele frequencies were calculated from HLA-A, -B, -C, and -DRB1 sequence data of 8862 potential stem cell donors registered with DKMS (German Bone Marrow Donor Registry) until June 2014. Donors were of self-assessed German origin. Allele frequencies were calculated to the two-field level (polypeptide sequence) (Schmidt et al., 2009). For allele frequency comparisons, chi-squared tests (Pearson, 1900) were applied in R (R Development Core Team, 2011). Pairwise proportion tests were made between the allele or haplotype frequencies, where $p < 0.05$ was considered significant. Omnibus tests for association with specific amino acid

positions, as well as pairwise tests for specific residues, were computed using the BIGDAWG R package (Pappas, Marin, Hollenbach, & Mack, 2016). Linear mixed effects modeling was performed using the Gaston package in R (<https://cran.r-project.org/web/packages/gaston/>) and the *lcMLkin* kinship matrix generated as above. Wilson Score Interval estimation was performed using the ‘Hmisc’ package of R (<https://CRAN.R-project.org/package=Hmisc>).

Reconstruction of *KIR* genotypes and *KIR* allele frequency analyses

Sequence reads specific to the *KIR* locus were identified by alignment to the human genome reference hg19 using BWA *mem*, and then extracting those mapping to chr19:55,228,188-55,383,188 or chr19_gl000209_random. The presence or absence and copy number of each *KIR* gene were determined using the PING pipeline (P.J. Norman et al., 2016), modified for single-end (SE; i.e. non-paired) reads. The alleles of *KIR3DL1/S1* were also determined using an SE modified version of PING, and further validated by determining the alleles of the genes flanking *KIR3DL1/S1* in the telomeric portion of the *KIR* locus. As an additional step, virtual sequence probes were used to identify specific alleles directly from FASTQ data files, with a threshold of ten reads used to positively identify a given allele. The scripts and probe sequences are available at <https://github.com/n0rmski/ThePlague/>.

References

- Abecasis, G. R., Auton, A., Brooks, L. D., DePristo, M. A., Durbin, R. M., Handsaker, R. E., . . . McVean, G. A. (2012). An integrated map of genetic variation from 1,092 human genomes. *Nature*, *491*(7422), 56–65. doi:10.1038/nature11632
- Abi-Rached, L., Dorigi, K., Norman, P. J., Yawata, M., & Parham, P. (2007). Episodes of natural selection shaped the interactions of IgA-Fc with FcαRI and bacterial decoy proteins. *J Immunol*, *178*(12), 7943–7954. doi:10.4049/jimmunol.178.12.7943
- Achkar, J. P., Klei, L., de Bakker, P. I. W., Bellone, G., Rebert, N., Scott, R., . . . Duerr, R. H. (2012). Amino acid position 11 of HLA-DR β 1 is a major determinant of chromosome 6p association with ulcerative colitis. *Genes and immunity*, *13*(3), 245–252. doi:10.1038/gene.2011.79
- Al Nabhani, Z., Dietrich, G., Hugot, J. P., & Barreau, F. Nod2: The intestinal gate keeper.

- (1553–7374 (Electronic)).
- Albright, F. S., Orlando, P., Pavia, A. T., Jackson, G. G., & Cannon Albright, L. A. (2008). Evidence for a heritable predisposition to death due to influenza. *J Infect Dis.*, 197(0022–1899 (Print)).
- Alexander, D. H., Novembre, J., & Lange, K. (2009). Fast model-based estimation of ancestry in unrelated individuals. *Genome Res.*, 19(9), 1655–1664.
- Alfirevic, A., Gonzalez-Galarza, F., Bell, C., Martinsson, K., Platt, V., Bretland, G., . . . Pirmohamed, M. (2012). In silico analysis of HLA associations with drug-induced liver injury: use of a HLA-genotyped DNA archive from healthy volunteers. *Genome Med*, 4(6), 51.
- Anand, P. K., Malireddi, R. K., Lukens, J. R., Vogel, P., Bertin, J., Lamkanfi, M., & Kanneganti, T. D. (2012). NLRP6 negatively regulates innate immunity and host defence against bacterial pathogens. *Nature*, 488(7411), 389–393. doi:10.1038/nature11250
- Andrades Valtuena, A., Mittnik, A., Massy, K., Allmae, R., Daubaras, M., Jankauskas, R., . . . Krause, J. (2016). The Stone Age Plague: 1000 years of Persistence in Eurasia. *bioRxiv*.
- Ankley, L., Thomas, S., & Olive, A. A.-O. (2020). Fighting Persistence: How Chronic Infections with Mycobacterium tuberculosis Evade T Cell-Mediated Clearance and New Strategies To Defeat Them. LID - e00916-19 [pii] LID - 10.1128/IAI.00916-19 [doi]. *Infect. Immun.*, 88(1098–5522 (Electronic)).
- Barreiro, L. B., Ben-Ali M Fau - Quach, H., Quach H Fau - Laval, G., Laval G Fau - Patin, E., Patin E Fau - Pickrell, J. K., Pickrell Jk Fau - Bouchier, C., . . . Quintana-Murci, L. (2009). Evolutionary dynamics of human Toll-like receptors and their different contributions to host defense. *PLoS Genet*, 5(1553–7404 (Electronic)).
- Bashirova, A. A., Martin, M. P., McVicar, D. W., & Carrington, M. (2006). The killer immunoglobulin-like receptor gene cluster: tuning the genome for defense. *Annu Rev Genomics Hum Genet*, 7, 277–300. doi:10.1146/annurev.genom.7.080505.115726
- Benedictow, O. J. (2004). *The Black Death, 1346–1353: The Complete History*, 383: Boydell & Brewer.
- Bhérrer, C., Campbell, C. L., & Auton, A. (2017). Refined genetic maps reveal sexual dimorphism in human meiotic recombination at multiple scales. *Nature Communications*, 8(1), 14994. doi:10.1038/ncomms14994
- Biraben, J.-N. (1976). *Les hommes et la peste en France et dans les pays européens et méditerranéens*. Mouton: Paris-La Haye.
- Bjorkman, P. J., & Parham, P. (1990). Structure, function, and diversity of class I major histocompatibility complex molecules. *Annu Rev Biochem*, 59, 253–288. doi:10.1146/annurev.bi.59.070190.001345
- Bos, K. I., Herbig, A., Sahl, J., Waglechner, N., Fourment, M., Forrest, S. A., . . . Poinar, H. N. (2016). Eighteenth century Yersinia pestis genomes reveal the long-term persistence of an historical plague focus. *Elife*, 5, e12994. doi:10.7554/eLife.12994

- Bos, K. I., Schuenemann, V. J., Golding, G. B., Burbano, H. A., Waglechner, N., Coombes, B. K., . . . Krause, J. (2011). A draft genome of *Yersinia pestis* from victims of the Black Death. *Nature*, *478*(7370), 506–510. doi:10.1038/nature10549
- Boudreau, J. E., & Hsu, K. C. (2018). Natural Killer Cell Education and the Response to Infection and Cancer Therapy: Stay Tuned. *Trends Immunol*, *39*(3), 222–239. doi:10.1016/j.it.2017.12.001
- Bowsky, W. M. (1971). *The Black Death: a turning point in history?*: New York, HOlt, Reinhart and Winston.
- Briggs, A. W., Stenzel, U., Johnson, P. L., Green, R. E., Kelso, J., Prufer, K., . . . Paabo, S. (2007). Patterns of damage in genomic DNA sequences from a Neandertal. *Proceedings of the National Academy of Sciences of the United States of America*, *104*(37), 14616–14621.
- Büntgen, U., Ginzler, C., Esper, J., Tegel, W., & McMichael, A. J. (2012). Digitizing historical plague. *Clin. Infect. Dis.*, *55*(11), 1586–1588.
- Cao, K., Hollenbach, J., Shi, X., Shi, W., Chopek, M., & Fernández-Viña, M. A. (2001). Analysis of the frequencies of HLA-A, B, and C alleles and haplotypes in the five major ethnic groups of the United States reveals high levels of diversity in these loci and contrasting distribution patterns in these populations. *Hum. Immunol.*, *62*(9), 1009–1030.
- Cedzynski, M., Nuytinck, L., Atkinson, A. P. M., St Swierzko, A., Zeman, K., Szemraj, J., . . . Kilpatrick, D. C. (2007). Extremes of L-ficolin concentration in children with recurrent infections are associated with single nucleotide polymorphisms in the FCN2 gene. *Clin. Exp. Immunol.*, *150*(1), 99–104.
- Clouse, M. (2002). *The Black Death Transformed: Disease and Culture in Early Renaissance Europe.*: Samuel K Cohn Jr. London and New York: Arnold and Oxford University Press, 2002, pp. 318, US\$65.00 (HB) ISBN: 0-340-70646-5. *International Journal of Epidemiology*, *31*(6), 1280–1281. doi:10.1093/ije/31.6.1280
- Cohn, S. K., Jr. (2003). *The Black Death Transformed: Disease and Culture in Early Renaissance Europe.* London: Edward Arnold.
- Danecek, P., Auton, A., Abecasis, G., Albers, C. A., Banks, E., DePristo, M. A., . . . Genomes Project Analysis, G. (2011). The variant call format and VCFtools. *Bioinformatics*, *27*(15), 2156–2158.
- Darke, C., Guttridge, M. G., Thompson, J., MacNamara, S., Street, J., & Thomas, M. (1998). HLA class I (A, B) and II (DR, DQ) gene and haplotype frequencies in blood donors from Wales. *Exp Clin Immunogenet*, *15*, 69–83.
- Dean, M., Carrington, M., Winkler, C., Huttley, G. A., Smith, M. W., Allikmets, R., . . . O'Brien, S. J. (1996). Genetic restriction of HIV-1 infection and progression to AIDS by a deletion allele of the CKR5 structural gene. Hemophilia Growth and Development Study, Multicenter AIDS Cohort Study, Multicenter Hemophilia Cohort Study, San Francisco City Cohort, ALIVE Study. *Science*, *273*(5283), 1856–1862.
- Di Marco, M., Schuster, H., Backert, L., Ghosh, M., Rammensee, H. G., & Stevanovic, S.

- (2017). Unveiling the Peptide Motifs of HLA-C and HLA-G from Naturally Presented Peptides and Generation of Binding Prediction Matrices. *J Immunol*, 199(8), 2639–2651. doi:10.4049/jimmunol.1700938
- Doherty, P. C., & Zinkernagel, R. M. (1975). A biological role for the major histocompatibility antigens. *Lancet*, 1(7922), 1406–1409.
- Drummond, W. K., Nelson, C. A., Fowler, J., Epton, E. E., Mead, P. S., & Lawaczek, E. W. (2014). Plague in a Pediatric Patient: Case Report and Use of Polymerase Chain Reaction as a Diagnostic Aid. *J Pediatric Infect Dis Soc*, 3(4), e38–41. doi:10.1093/jpids/piu001
- Dubaniewicz, A., Lewko, B., Moszkowska, G., Zamorska, B., & Stepinski, J. (2000). Molecular subtypes of the HLA-DR antigens in pulmonary tuberculosis. *Int. J. Infect. Dis.*, 4(3), 129–133.
- Dunne, C., Crowley, J., Hagan, R., Rooney, G., & Lawlor, E. (2008). HLA-A, B, Cw, DRB1, DQB1 and DPB1 alleles and haplotypes in the genetically homogenous Irish population. *Int. J. Immunogenet.*, 35(4–5), 295–302.
- Ell, S. R. (1984). Immunity as a Factor in the Epidemiology of Medieval Plague. *Reviews of Infectious Diseases*, 6(6), 866–879. doi:10.1093/clinids/6.6.866
- Ellwangen, S. (2007). *Die dunkle Zeit. Hexenverfolgung in der Stadt und Fürstpropstei Ellwangen*. Ellwangen: Stadtverwaltung Ellwangen.
- Everitt, A. R., Clare S Fau – Pertel, T., Pertel T Fau – John, S. P., John Sp Fau – Wash, R. S., Wash Rs Fau – Smith, S. E., Smith Se Fau – Chin, C. R., . . . Kellam, P. (2012). IFITM3 restricts the morbidity and mortality associated with influenza. *Nature*, 484(1476–4687 (Electronic)), 519–523. doi:D – NLM: EMS41068 FIR – Everingham, K
- Excoffier, L., & Lischer, H. E. L. (2010). Arlequin suite ver 3.5: a new series of programs to perform population genetics analyses under Linux and Windows. *Mol Ecol Resour*, 10(3), 564–567.
- Faul, F., Erdfelder, E., Lang, A.-G., & Buchner, A. (2007). G*Power 3: a flexible statistical power analysis program for the social, behavioral, and biomedical sciences. *Behav Res Methods*, 39(2), 175–191.
- Feldman, M., Harbeck, M., Keller, M., Spyrou, M. A., Rott, A., Trautmann, B., . . . Krause, J. (2016). A High-Coverage *Yersinia pestis* Genome from a Sixth-Century Justinianic Plague Victim. *Mol. Biol. Evol.*, 33(11), 2911–2923.
- Frisch, T., Sorensen, M. S., Overgaard, S., Lind, M., & Bretlau, P. (1998). Volume-Referent Bone Turnover Estimated From the Interlabel Area Fraction After Sequential Labeling. *Bone*, 22, 677–682. doi:10.1016/s8756-3282(98)00050-7
- Fu, Q., Meyer, M., Gao, X., Stenzel, U., Burbano, H. A., Kelso, J., & Pääbo, S. (2013). DNA analysis of an early modern human from Tianyuan Cave, China. *Proc. Natl. Acad. Sci. U.S.A.*, 110(6), 2223–2227.
- Fu, Q., Posth, C., Hajdinjak, M., Petr, M., Mallick, S., Fernandes, D., . . . Reich, D. (2016). The genetic history of Ice Age Europe. *Nature*, 534(7606), 200–205.
- Galvani, A. P., & Slatkin, M. (2003). Evaluating plague and smallpox as historical selective

- pressures for the CCR5-Delta 32 HIV-resistance allele. *Proceedings of the National Academy of Sciences of the United States of America*, 100(25), 15276–15279. doi:10.1073/pnas.2435085100
- Gnirke, A., Melnikov, A., Maguire, J., Rogov, P., LeProust, E. M., Brockman, W., . . . Nusbaum, C. (2009). Solution hybrid selection with ultra-long oligonucleotides for massively parallel targeted sequencing. *Nat Biotech*, 27(2), 182–189. doi:http://www.nature.com/nbt/journal/v27/n2/supinfo/nbt.1523_S1.html
- González-Neira, A., Calafell, F., Navarro, A., Lao, O., Cann, H., Comas, D., & Bertranpetit, J. (2004). Geographic stratification of linkage disequilibrium: a worldwide population study in a region of chromosome 22. *Hum. Genomics*, 1(6), 399–409.
- Gravel, Henn, B., Gutenkunst, R., Indap, A., Marth, G., Clark, A., . . . Project, T. G. (2011). Demographic history and rare allele sharing among human populations. *Proceedings of the National Academy of Sciences of the United States of America*, 108(29), 11983–11988. doi:10.1073/pnas.1019276108
- Guethlein, L. A., Norman, P. J., Hilton, H. G., & Parham, P. (2015). Co-evolution of MHC class I and variable NK cell receptors in placental mammals. *Immunol. Rev.*, 267(1), 259–282.
- Gumperz, J. E., Litwin, V., Phillips, J. H., Lanier, L. L., & Parham, P. (1995). The Bw4 public epitope of HLA-B molecules confers reactivity with natural killer cell clones that express NKB1, a putative HLA receptor. *J. Exp. Med.*, 181(3), 1133–1144.
- Guo, Y., Patil, N. K., Luan, L., Bohannon, J. K., & Sherwood, E. R. (2018). The biology of natural killer cells during sepsis. *Immunology*, 153(2), 190–202. doi:10.1111/imm.12854
- Haak, W., Lazaridis, I., Patterson, N., Rohland, N., Mallick, S., Llamas, B., . . . Reich, D. (2015). Massive migration from the steppe was a source for Indo-European languages in Europe. *Nature*, 522(7555), 207–211.
- Haller, B. C., & Messer, P. W. (2017). SLiM 2: Flexible, Interactive Forward Genetic Simulations. *Mol. Biol. Evol.*, 34(1), 230–240.
- Haller, B. C., & Messer, P. W. (2019). SLiM 3: Forward Genetic Simulations Beyond the Wright-Fisher Model. *Molecular Biology and Evolution*, 36(3), 632–637. doi:10.1093/molbev/msy228
- Hammer, C., Begemann, M., McLaren, P. J., Barth, A., Michel, A., Klose, B., . . . Fellay, J. (2015). Amino Acid Variation in HLA Class II Proteins Is a Major Determinant of Humoral Response to Common Viruses. *American journal of human genetics*, 97(5), 738–743. doi:10.1016/j.ajhg.2015.09.008
- Harrison, G. F., Sanz, J., Boulais, J., Mina, M. A.-O., Grenier, J. A.-O., Leng, Y., . . . Barreiro, L. B. (2019). Natural selection contributed to immunological differences between hunter-gatherers and agriculturalists. *Nature Ecology and Evolution*, 3(2397–334X (Electronic)), 1253–1264.
- Hellenthal, G., Busby, G. B., Band, G., Wilson, J. F., Capelli, C., Falush, D., & Myers, S. (2014). A genetic atlas of human admixture history. *Science*, 343(6172), 747–751.

- Hilton, H. G., Guethlein, L. A., Goyos, A. A.-O. X., Nemat-Gorgani, N., Bushnell, D. A., Norman, P. J., & Parham, P. (2015). Polymorphic HLA-C Receptors Balance the Functional Characteristics of KIR Haplotypes. *J Immunol*, *195*(1550–6606 (Electronic)), 160–170.
- Hoang, T. V., Toan, N. L., Song, L. H., Ouf, E. A., Bock, C. T., Kremsner, P. G., . . . Velavan, T. P. (2011). Ficolin-2 levels and FCN2 haplotypes influence hepatitis B infection outcome in Vietnamese patients. *PLoS ONE*, *6*(11), e28113.
- Holdsworth, R., Hurley, C. K., Marsh, S. G., Lau, M., Noreen, H. J., Kempenich, J. H., . . . Maier, M. (2009). The HLA dictionary 2008: a summary of HLA-A, -B, -C, -DRB1/3/4/5, and -DQB1 alleles and their association with serologically defined HLA-A, -B, -C, -DR, and -DQ antigens. *Tissue Antigens*, *73*(2), 95–170. doi:10.1111/j.1399-0039.2008.01183.x
- Hollenbach, J., Ncedal, I., Ladner, M. B., Single, R. M., & Trachtenberg, E. A. (2012). Killer cell immunoglobulin-like receptor (KIR) gene content variation in the HGDP-CEPH populations. *Immunogenetics*. doi:10.1007/s00251-012-0629-x
- Hollenbach, J., Norman, P. J., Creary, L. E., Damotte, V. A.-O., Montero-Martin, G., Caillier, S., . . . Oksenberg, J. R. (2019). A specific amino acid motif of HLA-DRB1 mediates risk and Interacts with smoking history in Parkinson's Disease. *Proc. Natl. Acad. Sci. U.S.A.*, *116*(1091–6490 (Electronic)), 7419–7424.
- Hummelshoj, T., Munthe-Fog, L., Madsen, H. O., Fujita, T., Matsushita, M., & Garred, P. (2005). Polymorphisms in the FCN2 gene determine serum variation and function of Ficolin-2. *Hum. Mol. Genet.*, *14*(12), 1651–1658.
- Huson, D. H., Auch, A. F., Qi, J., & Schuster, S. C. (2007). MEGAN analysis of metagenomic data. *Genome Res.*, *17*(3), 377–386.
- Inohara, Chamailard, McDonald, C., & Nunez, G. (2005). NOD-LRR proteins: role in host-microbial interactions and inflammatory disease. *Annu Rev Biochem*, *74*, 355–383. doi:10.1146/annurev.biochem.74.082803.133347
- Johansson, A., Ingman, M., Mack, S. J., Ehrlich, H., & Gyllensten, U. (2008). Genetic origin of the Swedish Sami inferred from HLA class I and class II allele frequencies. *Eur J Hum Genet.*, *16*, 1341–1349.
- Jonsson, H., Ginolhac, A., Schubert, M., Johnson, P. L., & Orlando, L. (2013). mapDamage2.0: fast approximate Bayesian estimates of ancient DNA damage parameters. *Bioinformatics*, *29*(13), 1682–1684.
- Kairies, M.-S. (2015). *Drei frühneuzeitliche Massengräber aus Ellwangen (Jagst) – Paläopathologie und demographische Struktur*. (Master of Science), University of Tübingen, Germany.
- Karlsson, E. K., Harris Jb Fau – Tabrizi, S., Tabrizi S Fau – Rahman, A., Rahman A Fau – Shlyakhter, I., Shlyakhter I Fau – Patterson, N., Patterson N Fau – O'Dushlaine, C., . . . Larocque, R. C. (2013). Natural selection in a bangladeshi population from the cholera-endemic ganges river delta. *Sci Transl Med.*, *5*(1946–6242 (Electronic)).
- Keller, M., Spyrou, M. A., Scheib, C. L., Neumann, G. U., Kröpelin, A., Haas-Gebhard,

- B., . . . Krause, J. (2019). Ancient genomes from across Western Europe reveal early diversification during the First Pandemic (541–750). *Proc. Natl. Acad. Sci. U.S.A.*, *116*(25), 12363–12372.
- Key, F. M., Fu, Q., Romagné, F., Lachmann, M., & Andrés, A. M. (2016). Human adaptation and population differentiation in the light of ancient genomes. *Nat Commun*, *7*, 10775.
- Key, F. M., Peter, B., Dennis, M. Y., Huerta-Sánchez, E., Tang, W., Prokunina-Olsson, L., . . . Andrés, A. M. (2014). Selection on a variant associated with improved viral clearance drives local, adaptive pseudogenization of interferon lambda 4 (IFNL4). (1553–7404 (Electronic)).
- Kim, S., Sunwoo, J. B., Yang, L., Choi, T., Song, Y.-J., French, A. R., . . . Yokoyama, W. M. (2008). HLA alleles determine differences in human natural killer cell responsiveness and potency. *Proceedings of the National Academy of Sciences of the United States of America*, *105*(8), 3053–3058. doi:10.1073/pnas.0712229105
- Kircher, M., Sawyer, S., & Meyer, M. (2012). Double indexing overcomes inaccuracies in multiplex sequencing on the Illumina platform. *Nucleic Acids Res*, *40*(1), e3.
- Klebanov, N. (2018). Genetic Predisposition to Infectious Disease. *Cureus*, *10*(8), e3210.
- Korneliussen, T. S., Albrechtsen, A., & Nielsen, R. (2014). ANGSD: Analysis of Next Generation Sequencing Data. *BMC Bioinformatics*, *15*, 356.
- Kwiatkowski, D. P. (2005). How malaria has affected the human genome and what human genetics can teach us about malaria. *Am. J. Hum. Genet.*, *77*(0002–9297 (Print)), 171–192.
- Laayouni, H., Oosting, M., Luisi, P., Ioana, M., Alonso, S., Ricaño-Ponce, I., . . . Netea, M. G. (2014). Convergent evolution in European and Roma populations reveals pressure exerted by plague on Toll-like receptors. *Proc. Natl. Acad. Sci. U.S.A.*, *111*(7), 2668–2673.
- Lamkanfi, M., & Dixit, V. M. (2014). Mechanisms and functions of inflammasomes. *Cell*, *157*(5), 1013–1022. doi:10.1016/j.cell.2014.04.007
- Lamnidis, T. C., Majander, K., Jeong, C., Salmela, E., Wessman, A., Moiseyev, V., . . . Schiffels, S. (2018). Ancient Fennoscandian genomes reveal origin and spread of Siberian ancestry in Europe. *Nat Commun*, *9*(1), 5018. doi:10.1038/s41467-018-07483-5
- Lazaridis, I., Patterson, N., Mitnik, A., Renaud, G., Mallick, S., Kirsanow, K., . . . Krause, J. (2014). Ancient human genomes suggest three ancestral populations for present-day Europeans. *Nature*, *513*(7518), 409–413.
- Lenski, R. E. (1988). Evolution of plague virulence. *Nature*, *334*(6182), 473–474.
- Li, H. (2011). A statistical framework for SNP calling, mutation discovery, association mapping and population genetical parameter estimation from sequencing data. *Bioinformatics*, *27*(21), 2987–2993.
- Li, H., & Durbin, R. (2010). Fast and accurate long-read alignment with Burrows-Wheeler transform. *Bioinformatics*, *26*(5), 589–595.
- Li, H., Handsaker, B., Wysoker, A., Fennell, T., Ruan, J., Homer, N., . . . Genome Project

- Data Processing, S. (2009). The Sequence Alignment/Map format and SAMtools. *Bioinformatics*, 25(16), 2078–2079.
- Lindo, J., Huerta-Sánchez, E., Nakagome, S., Rasmussen, M., Petzelt, B., Mitchell, J., . . . Malhi, R. S. (2016). A time transect of exomes from a Native American population before and after European contact. *Nat Commun*, 7, 13175.
- Lipatov, M., Sanjeev, K., Patro, R., & Veeramah, K. (2015). Maximum Likelihood Estimation of biological Relatedness from low Coverage Sequencing Data. *bioRxiv*.
- Long, E. O., Kim, H. S., Liu, D., Peterson, M. E., & Rajagopalan, S. (2013). Controlling natural killer cell responses: integration of signals for activation and inhibition. *Annu Rev Immunol*, 31, 227–258. doi:10.1146/annurev-immunol-020711-075005
- Luo, F., Sun, X., Wang, Y., Wang, Q., Wu, Y., Pan, Q., . . . Zhang, X.-L. (2013). Ficolin-2 defends against virulent Mycobacteria tuberculosis infection in vivo, and its insufficiency is associated with infection in humans. *PLoS ONE*, 8(9), e73859.
- Martinon, F., Burns, K., & Tschopp, J. (2002). The inflammasome: a molecular platform triggering activation of inflammatory caspases and processing of proIL-beta. *Mol Cell*, 10(2), 417–426.
- Mathieson, I., Lazaridis, I., Rohland, N., Mallick, S., Patterson, N., Roodenberg, S. A., . . . Reich, D. (2015). Genome-wide patterns of selection in 230 ancient Eurasians. *Nature*, 528(7583), 499–503.
- McManus, K. A.-O., Taravella, A. M., Henn, B. A.-O. X., Bustamante, C. D., Sikora, M., & Cornejo, O. A.-O. (2017). Population genetic analysis of the DARC locus (Duffy) reveals adaptation from standing variation associated with malaria resistance in humans. *PLoS Genet*, 13(1553–7404 (Electronic)).
- McVicker, G., Gordon, D., Davis, C., & Green, P. (2009). Widespread genomic signatures of natural selection in hominid evolution. *PLoS Genet.*, 5(5), e1000471.
- Meyer, M., & Kircher, M. (2010). Illumina sequencing library preparation for highly multiplexed target capture and sequencing. *Cold Spring Harb Protoc*, 2010(6), pdb.prot5448.
- Monroy, K., Jose, M., Jakobsson, M., & Günther, T. (2017). Estimating genetic Kin Relationships in prehistoric Populations. *bioRxiv*.
- Morelli, G., Song, Y., Mazzoni, C. J., Eppinger, M., Roumagnac, P., Wagner, D. M., . . . Achtman, M. (2010). Yersinia pestis genome sequencing identifies patterns of global phylogenetic diversity. *Nat. Genet.*, 42(12), 1140–1143.
- Namouchi, A., Guellil, M., Kersten, O., Hänsch, S., Ottoni, C., Schmid, B. V., . . . Bramanti, B. (2018). Integrative approach using Yersinia pestis genomes to revisit the historical landscape of plague during the Medieval Period. *Proceedings of the National Academy of Sciences*, 115(50), E11790. doi:10.1073/pnas.1812865115
- Neefjes, J., Jongsma, M. L. M., Paul, P., & Bakke, O. (2011). Towards a systems understanding of MHC class I and MHC class II antigen presentation. *Nat. Rev. Immunol.*, 11(12), 823–836.
- Norman, P. J., Hollenbach, J., Nemat-Gorgani, N., Marin, W., Norberg, S., Ashouri, E., . . .

- Parham, P. (2016). Defining KIR and HLA Class I Genotypes at Highest Resolution via High-Throughput Sequencing. *Am. J. Hum. Genet.*, 99(2), 375–391.
- Norman, P. J., Norberg, S. J., Guethlein, L. A., Nemat-Gorgani, N., Royce, T., Wroblewski, E. E., . . . Parham, P. (2017). Sequences of 95 human MHC haplotypes reveal extreme coding variation in genes other than highly polymorphic HLA class I and II. *Genome Res*, 27(5), 813–823. doi:10.1101/gr.213538.116
- Nowak, J., Mika-Witkowska, R., Polak, M., Zajko, M., Rogatko-Koros, M., Graczyk-Pol, E., & Lange, A. (2008). Allele and extended haplotype polymorphism of HLA-A, -C, -B, -DRB1 and -DQB1 loci in Polish population and genetic affinities to other populations. *Tissue Antigens*, 71(3), 193–205. doi:10.1111/j.1399-0039.2007.00991.x
- Ogawa, K., & Okada, Y. (2020). The current landscape of psoriasis genetics in 2020. *J Dermatol Sci.*, S0923-1811(1873-569X (Electronic)). doi:10.1016/j.jdermsci.2020.05.008
- Pappas, D. J., Marin, W., Hollenbach, J. A., & Mack, S. J. (2016). Bridging ImmunoGenomic Data Analysis Workflow Gaps (BIGDAWG): An integrated case-control analysis pipeline. *Hum. Immunol.*, 77(3), 283–287.
- Parham, P., & Moffett, A. (2013). Variable NK cell receptors and their MHC class I ligands in immunity, reproduction and human evolution. *Nat Rev Immunol*, 13(2), 133–144. doi:10.1038/nri3370
- Park, Y. H., Remmers, E. A.-O., Lee, W. A.-O., Ombrello, A. K., Chung, L. K., Shilei, Z., . . . Chae, J. A.-O. (2020). Ancient familial Mediterranean fever mutations in human pyrin and resistance to *Yersinia pestis*. *Nat Immunol.*, 21(1529–2916 (Electronic)), 857–867.
- Patin, E., Lopez, M., Grollemund, R., Verdu, P., Harmant, C., Quach, H., . . . Quintana-Murci, L. (2017). Dispersals and genetic adaptation of Bantu-speaking populations in Africa and North America. *Science*, 356(6337), 543–546. doi:10.1126/science.aal1988
- Patterson, N., Moorjani, P., Luo, Y., Mallick, S., Rohland, N., Zhan, Y., . . . Reich, D. (2012). Ancient admixture in human history. *Genetics*, 192(3), 1065–1093.
- Patterson, N., Price, A. L., & Reich, D. (2006). Population structure and eigenanalysis. *PLoS Genet.*, 2(12), e190.
- Pearson, K. (1900). On the criterion that a given system of deviations from the probable in the case of a correlated system of variables is such that it can be reasonably supposed to have arisen from random sampling. *Philosophical Magazine Series 5*, 50, 157–175. doi:10.1080/14786440009463897
- Peltzer, A., Jäger, G., Herbig, A., Seitz, A., Knip, C., Krause, J., & Nieselt, K. (2016). EAGER: efficient ancient genome reconstruction. *Genome Biol.*, 17(60). doi:10.1186/s13059-016-0918-z
- Philip, N. H., Zwack, E. E., & Brodsky, I. E. (2016). Activation and Evasion of Inflammasomes by *Yersinia*. *Curr Top Microbiol Immunol*, 397, 69–90. doi:10.1007/978-3-319-41171-2_4
- Pieters, J. (2008). *Mycobacterium tuberculosis* and the macrophage: maintaining a balance.

- Cell Host Microbe*, 3(6), 399–407.
- Pingel, J., Solloch, U. V., Hofmann, J. A., Lange, V., Ehninger, G., & Schmidt, A. H. (2013). High-resolution HLA haplotype frequencies of stem cell donors in Germany with foreign parentage: how can they be used to improve unrelated donor searches? *Hum. Immunol.*, 74(3), 330–340.
- Pinhasi, R., Fernandes, D., Sirak, K., Novak, M., Connell, S., Alpaslan-Roodenberg, S., . . . Hofreiter, M. (2015). Optimal Ancient DNA Yields from the Inner Ear Part of the Human Petrous Bone. *PLoS ONE*, 10(6), e0129102. doi:10.1371/journal.pone.0129102
- Politzer, R., & WHO. (1954). *Plague*.
- Prugnolle, F., Manica, A., Charpentier, M., Guégan, J., V., G., & Balloux, F. (2005). Pathogen-driven selection and worldwide HLA class I diversity. *Current Biology*, 15, 1022–1027.
- Quinlan, A. R. (2014). BEDTools: The Swiss-Army Tool for Genome Feature Analysis. *Curr Protoc Bioinformatics*, 47, 11.12.11–34. doi:10.1002/0471250953.bi1112s47
- Quintana-Murci, L. (2019). Human Immunology through the Lens of Evolutionary Genetics. *Cell*, 177(1), 184–199. doi:10.1016/j.cell.2019.02.033
- R Development Core Team. (2011). *R: A Language and Environment for Statistical Computing*. Vienna, Austria : the R Foundation for Statistical Computing: R Foundation for Statistical Computing.
- Radwan, J., Babik, W., Kaufman, J., Lenz, T. L., & Winternitz, J. (2020). Advances in the Evolutionary Understanding of MHC Polymorphism. *Trends in Genetics*, 36, 298–311.
- Ralph, P. L., & Coop, G. (2015). Convergent Evolution During Local Adaptation to Patchy Landscapes. *PLoS Genet.*, 11(11), e1005630.
- Rascovan, N., Sjögren, K.-G., Kristiansen, K., Nielsen, R., Willerslev, E., Desnues, C., & Rasmussen, S. (2019). Emergence and Spread of Basal Lineages of *Yersinia pestis* during the Neolithic Decline. *Cell*, 176(1–2), 295–305.e210.
- Rasmussen, S., Allentoft, M. E., Nielsen, K., Orlando, L., Sikora, M., Sjögren, K. G., . . . Willerslev, E. (2015). Early divergent strains of *Yersinia pestis* in Eurasia 5,000 years ago. *Cell*, 163(3), 571–582. doi:10.1016/j.cell.2015.10.009
- Renaud, G., Slon, V., Duggan, A. T., & Kelso, J. (2015). Schmutzi: estimation of contamination and endogenous mitochondrial consensus calling for ancient DNA. *Genome Biology*, 16(1), 224. doi:10.1186/s13059-015-0776-0
- Robinson, J., Halliwell, J. A., Hayhurst, J. D., Flicek, P., Parham, P., & Marsh, S. G. E. (2015). The IPD and IMGT/HLA database: allele variant databases. *Nucleic Acids Res.*, 43(Database issue), D423–D431.
- Robinson, J., Thorvaldsdóttir, H., Winckler, W., Guttman, M., Lander, E. S., Getz, G., & Mesirov, J. P. (2011). Integrative genomics viewer. *Nat. Biotechnol.*, 29(1), 24–26.
- Rohland, N., Harney, E., Mallick, S., Nordenfelt, S., & Reich, D. (2015). Partial uracil-DNA-glycosylase treatment for screening of ancient DNA. *Philos Trans R Soc Lond B Biol Sci*, 370(1660), 20130624. doi:10.1098/rstb.2013.0624
- Rohland, N., & Hofreiter, M. (2007). Ancient DNA extraction from bones and teeth. *Nat*

- 1173 *Protoc*, 27), 1756–1762.
- 1174 Sabeti, Schaffner, S., Fry, B., Lohmueller, J., Varilly, P., Shamovsky, O., . . . Lander, E. S.
 1175 (2006). Positive natural selection in the human lineage. *Science*, 312(5780), 1614–
 1176 1620. doi:10.1126/science.1124309
- 1177 Sabeti, Varilly, P., Fry, B., Lohmueller, J., Hostetter, E., Cotsapas, C., . . . Stewart, J.
 1178 (2007). Genome-wide detection and characterization of positive selection in human
 1179 populations. *Nature*, 449(1476–4687 (Electronic)), 913–918. doi:D – NLM: UKMS4416
 1180 EDAT– 2007/10/19 09:00 MHDA– 2007/12/06 09:00 CRDT– 2007/10/19 09:00
 1181 PHST– 2007/08/08 00:00 [received] PHST– 2007/09/13 00:00 [accepted] PHST–
 1182 2007/10/19 09:00 [pubmed] PHST– 2007/12/06 09:00 [medline] PHST– 2007/10/19
 1183 09:00 [entrez] AID – nature06250 [pii] AID – 10.1038/nature06250 [doi] PST –
 1184 ppublish
- 1185 Saunders, P. M., Vivian, J. P., O'Connor, G. M., Sullivan, L. C., Pymm, P., Rossjohn, J., &
 1186 Brooks, A. G. (2015). A bird's eye view of NK cell receptor interactions with their
 1187 MHC class I ligands. *Immunol Rev*, 267(1), 148–166. doi:10.1111/imr.12319
- 1188 Schmidt, A. H., Baier, D., Solloch, U. V., Stahr, A., Cereb, N., Wassmuth, R., . . . Rutt, C.
 1189 (2009). Estimation of high-resolution HLA-A, -B, -C, -DRB1 allele and haplotype
 1190 frequencies based on 8862 German stem cell donors and implications for strategic
 1191 donor registry planning. *Hum. Immunol.*, 70(11), 895–902.
- 1192 Skoglund, P., Storå, J., Götherström, A., & Jakobsson, M. (2013). Accurate sex identification
 1193 of ancient human remains using DNA shotgun sequencing. *Journal of Archaeological
 1194 Science*, 40(12), 4477–4482.
- 1195 Solloch, U. V., Lang, K., Lange, V., Böhme, I., Schmidt, A. H., & Sauter, J. (2017).
 1196 Frequencies of gene variant CCR5-Δ32 in 87 countries based on next-generation
 1197 sequencing of 1.3 million individuals sampled from 3 national DKMS donor centers.
 1198 *Hum. Immunol.*, 78(11–12), 710–717.
- 1199 Spyrou, M. A., Keller, M., Tukhbatova, R. I., Scheib, C. L., Nelson, E. A., Andrades
 1200 Valtueña, A., . . . Krause, J. (2019). Phylogeography of the second plague pandemic
 1201 revealed through analysis of historical *Yersinia pestis* genomes. *Nature
 1202 Communications*, 10(1), 4470–4470. doi:10.1038/s41467-019-12154-0
- 1203 Spyrou, M. A., Tukhbatova, R. I., Feldman, M., Drath, J., Kacki, S., Beltran de Heredia,
 1204 J., . . . Krause, J. (2016). Historical *Y. pestis* Genomes Reveal the European Black
 1205 Death as the Source of Ancient and Modern Plague Pandemics. *Cell Host Microbe*,
 1206 19(6), 874–881. doi:10.1016/j.chom.2016.05.012
- 1207 Spyrou, M. A., Tukhbatova, R. I., Wang, C.-C., Valtueña, A. A., Lankapalli, A. K.,
 1208 Kondrashin, V. V., . . . Krause, J. (2018). Analysis of 3800-year-old *Yersinia pestis*
 1209 genomes suggests Bronze Age origin for bubonic plague. *Nat Commun*, 9(1), 2234.
- 1210 Stephens, J. C., Reich, D. E., Goldstein, D. B., Shin, H. D., Smith, M. W., Carrington,
 1211 M., . . . Dean, M. (1998). Dating the origin of the CCR5-Delta32 AIDS-resistance
 1212 allele by the coalescence of haplotypes. *Am. J. Hum. Genet.*, 62(6), 1507–1515.
- 1213 Sun, J., Yang, C., Fei, W., Zhang, X., Sheng, Y., Zheng, X., . . . Zhang, X. (2018). HLA-

- DQ β 1 amino acid position 87 and DQB1*0301 are associated with Chinese Han SLE. *Molecular genetics & genomic medicine*, 6(4), 541–546. doi:10.1002/mgg3.403
- Szolek, A., Schubert, B., Mohr, C., Sturm, M., Feldhahn, M., & Kohlbacher, O. (2014). OptiType: precision HLA typing from next-generation sequencing data. *Bioinformatics*, 30(23), 3310–3316. doi:10.1093/bioinformatics/btu548
- The Genome Sequencing Consortium. (2001). Initial sequencing and analysis of the human genome. *Nature*, 409(6822), 860–921.
- Trowsdale, J., & Knight, J. C. (2013). Major histocompatibility complex genomics and human disease. *Annu Rev Genomics Hum Genet*, 14, 301–323.
- Uhrberg, M., Valiante, N. M., Shum, B. P., Shilling, H. G., Lienert-Weidenbach, K., Corliss, B., . . . Parham, P. (1997). Human diversity in killer cell inhibitory receptor genes. *Immunity*, 7(6), 753–763.
- Vågene, Å. J., Herbig, A., Campana, M. G., Robles García, N. M., Warriner, C., Sabin, S., . . . Krause, J. (2018). Salmonella enterica genomes from victims of a major sixteenth-century epidemic in Mexico. *Nature Ecology & Evolution*, 2, 520–528.
- Vasseur, E., Boniotto, M., Patin, E., Laval, G., Quach, H., Manry, J., . . . Quintana-Murci, L. (2012). The evolutionary landscape of cytosolic microbial sensors in humans. *American journal of human genetics*, 91(1), 27–37. doi:10.1016/j.ajhg.2012.05.008
- Vladimer, G. I., Marty-Roix, R., Ghosh, S., Weng, D., & Lien, E. (2013). Inflammasomes and host defenses against bacterial infections. *Curr Opin Microbiol*, 16(1), 23–31. doi:10.1016/j.mib.2012.11.008
- Vladimer, G. I., Weng, D., Paquette, S. W., Vanaja, S. K., Rathinam, V. A., Aune, M. H., . . . Lien, E. (2012). The NLRP12 inflammasome recognizes *Yersinia pestis*. *Immunity*, 37(1), 96–107. doi:10.1016/j.immuni.2012.07.006
- Voight, B. F., Kudaravalli, S., Wen, X., & Pritchard, J. K. (2006). A map of recent positive selection in the human genome. *PLoS Biol.*, 4(1545–7885 (Electronic)).
- Wagner, D. M., Klunk, J., Harbeck, M., Devault, A., Waglechner, N., Sahl, J. W., . . . Poinar, H. (2014). *Yersinia pestis* and the plague of Justinian 541–543 AD: a genomic analysis. *Lancet Infect Dis*, 14(4), 319–326. doi:10.1016/s1473-3099(13)70323-2
- Wang, E. T., Kodama, G., Baldi, P., & Moyzis, R. K. (2006). Global landscape of recent inferred Darwinian selection for *Homo sapiens*. *Proc. Natl. Acad. Sci. U.S.A.*, 103(0027–8424 (Print)), 135–140.
- Weese, D., Holtgrewe, Manuel, & Reinert, K. (2012). RazerS 3: Faster, fully sensitive read mapping. *Bioinformatics*. doi:10.1093/bioinformatics/bts505
- Weir, B. S., & Cockerham, C. C. (1984). ESTIMATING F-STATISTICS FOR THE ANALYSIS OF POPULATION STRUCTURE. (1558–5646 (Electronic)).
- WHO. (2017). Plague in Madagascar. *WHO*.
- Wilson, M. J., Torkar, M., Haude, A., Milne, S., Jones, T., Sheer, D., . . . Trowsdale, J. (2000). Plasticity in the organization and sequences of human KIR/ILT gene families. *Proceedings of the National Academy of Sciences of the United States of America*, 97(9), 4778–4783. doi:10.1073/pnas.080588597

Zaki, M. H., Man, S. M., Vogel, P., Lamkanfi, M., & Kanneganti, T. D. (2014). Salmonella exploits NLRP12-dependent innate immune signaling to suppress host defenses during infection. *Proceedings of the National Academy of Sciences of the United States of America*, 111(1), 385–390. doi:10.1073/pnas.1317643111

Acknowledgements

We thank Almut Nebel for her advice to assess the statistical power and the obtainable effect sizes from our given sample. Our special thanks goes to Karl Hilsenbek and Theresa Hilsenbek for the announcement of our project to the inhabitants and students of Ellwangen, and so, for conferring the collection of anonymous saliva samples. In this context we want to deeply thank all participants from Ellwangen who contributed their anonymous saliva samples to make this study possible. We also thank Michael Franken for sampling the Ellwangen plague individuals for petrous bones. Thanks to Chris Gignoux for advice on data analysis. This work was supported by the European Research Council (APGREID) and NIH/NIAID R56 AI151549 (to PJ Norman).

Ethical Approval for modern and ancient Samples

Saliva samples were obtained from the contributing persons after their consent was given. The samples were obtained in a completely anonymised way, so that no personal information was registered. Ethical Approval was granted by the Ethics Committee of the Faculty of Medicine of the Eberhard Karls University and the University Hospital of Tübingen. According to ethical guidelines, sampling of 16th century teeth and petrous bones was performed with archaeological / anthropological supervision to minimize the destructive effect. Each sample was sampled only once and photographs were taken before and after the sampling procedure. Every sample has been documented and archived in the aDNA facility of the Max Planck Institute for the Science of Human History in Jena, Germany.

Author Contributions

AI, AS, PJN, AH, KIB, SF, OK and JK designed the immunity capture. AI, ER and JK collected modern saliva samples. AI, MAS, VJS and ER conducted lab work. AI, RB, AS and DIHZ performed HLA genotyping, and FMK conducted *D_{Anc}* and *F_{st}* analysis. JS and BKK performed pathogen screening. PJN and MKR performed KIR genotyping. JH and PJN performed data

analyses. PJN, WHP and GFH performed simulations for natural selection. JS, US and AHS contributed the DKMS allele frequencies. RW and SA led the Excavation in Ellwangen. JW and RW provided the 16th century Ellwangen samples. MSK and JW conducted anthropological analyses. AI, JH, PJN and JK wrote the manuscript. JK led the study.

Conflicts of Interests

The authors declare no conflicts of interests.

Data Availability

The data underlying this article is available on the European Nucleotide Archive under the accession number PRJEB44124 (ERP128137).

Figures



Figure 1. Mass burials discovered at Ellwangen. A. Location of Ellwangen in Germany. B. Location of the marketplace, where the mass burials were discovered during an excavation in 2013-2015. C. Mass grave 549 showing several individuals being buried together.

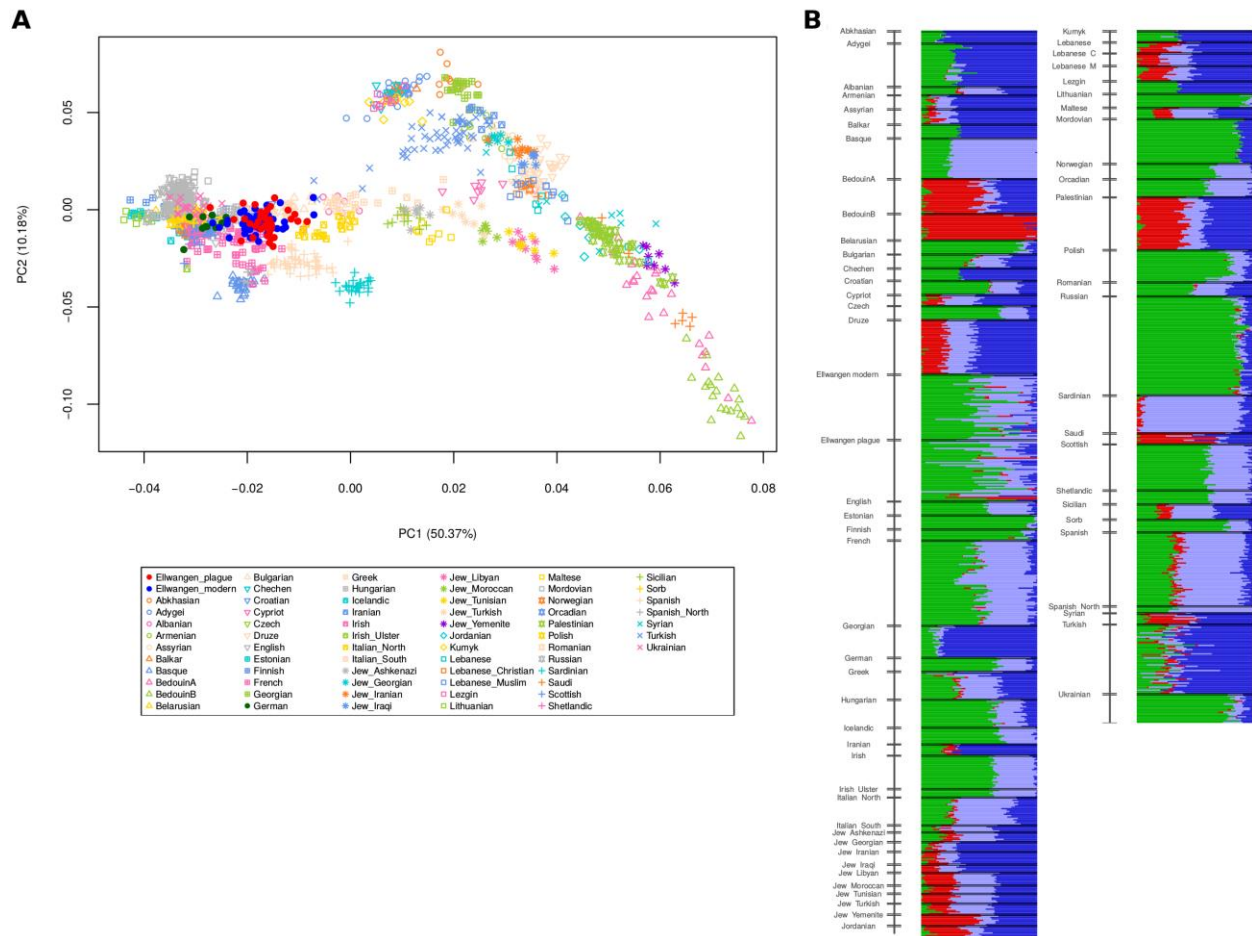


Figure 2. The 16th century plague victims and modern inhabitants of Ellwangen form a continuous population

A. PCA showing the 16th century (red) and modern (blue) Ellwangen populations in the context of 65 modern day populations from West-Eurasia based on 1,233,013 genome wide SNPs (Lazaridis et al. 2014; Haak et al. 2015; Fu et al. 2016). **B.** Admixture modeling based on four ancestral components (K=4) of the same 65 modern West Eurasian populations including 16th century (Ellwangen plague) and modern Ellwangen (Ellwangen modern) populations. The K=4 model was chosen due to the lowest cross-validation error.

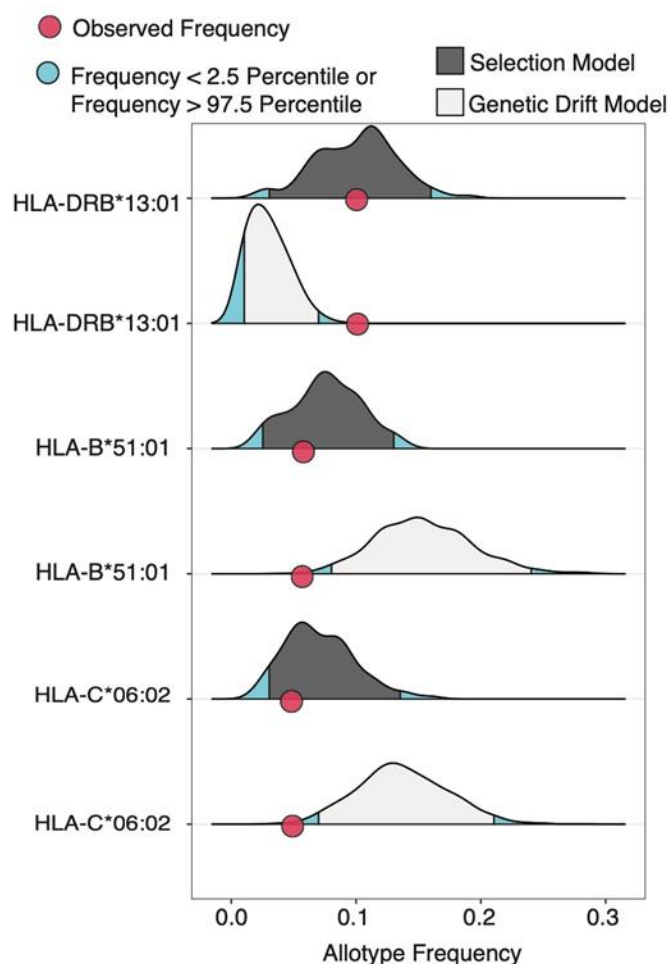


Figure 3. Natural selection drives HLA allele frequency changes

Density plots showing the distributions of allele frequencies from SLIM3 model simulations with (dark grey) or without (light grey) natural selection. The starting frequency for simulations was the observed frequency in the 16th century population. Selection coefficients for the models with natural selection were -0.1 for *HLA-B*51:01* and *HLA-C*06:02* and 0.2 for *DRB1*13:01* (Supplementary Figure 5). The 2.5% extremes are shown in blue illustrating where the p-value cut-off of 0.05 would occur. Red points represent the frequency in the modern-day population.

Table 1. Genes identified in the 0.01% tail of distribution following *DAnC* analysis. **Ref** = reference, **Alt** = alternative, **Der** = derived, **Anc** = derived allele frequency in Ellwangen 16th century, **Mod** = derived allele frequency in Ellwangen modern, **CEU** = derived allele frequency in Central Europeans from Utah, **FIN** = derived allele frequency in Finnish, **GBR** = derived

allele frequency in Great Britains (obtained from the 1000 Genomes Project Phase 3 data). Red text indicates alleles that have significantly ($p < 0.05$) increased in frequency in the modern individuals and blue text indicates that allele frequency has significantly ($p < 0.05$) decreased in frequency in the modern individuals. F_{ST} empirical p-value refers to the empirical distribution of F_{ST} calculated between the 16th century and the modern Ellwangen population.

Chromosome			Allele			Ellwangen										
No.	Position	SNP ID	Ref	Alt	Der	Anc	Mod	CEU	FIN	GBR	DAnc	F _{ST} empirical p-value	Variant	Gene	Function	
9	137772664	rs17514136	A	G	G	0.17	0.37	0.28	0.24	0.21	0.20	0.99	5_prime_UTR	FCN2	activation of the lectin complement pathway	
9	137779026	rs17549193	C	T	T	0.19	0.39	0.29	0.25	0.23	0.20	0.99	missense	FCN2		
11	7079038	rs10839708	G	A	A	0.69	0.51	0.60	0.65	0.63	0.18	0.97	missense	NLRP14	activation of pro- inflammatory caspases	

Table 2. Genotype and allele frequencies of *CCR5*-wildtype (wt), and *CCR5-Δ32* ($\Delta 32$), among the plague victims and modern individuals from Ellwangen. The individual genotypes are given in Supplementary Data 6A. The frequencies for Germany were obtained from a study of German bone marrow donor registry volunteers (Solloch et al., 2017) for comparison.

	Genotype frequency (%)			Allele Frequency (%)	
	wt/wt	wt/ $\Delta 32$	$\Delta 32/\Delta 32$	wt	$\Delta 32$
Ellwangen plague	71.4	23.8	4.8	83.4	16.6
Ellwangen modern	78.4	21.6	0	89.2	10.8
Germany	79.2	19.4	1.4	88.8	11.2

Table 3. *HLA-B*, *-C* and *-DRB1* allele frequencies in 16th century plague victims and modern inhabitants of Ellwangen. Frequency differences with $p < 0.05$ are highlighted in red. No significance could be obtained after multiple testing correction (for details see Supplementary Data 5A).

Locus	Frequency (%) Plague	Frequency (%) Modern	P-value
B*07:02	13.89	14	0.984
B*08:01	9.72	13	0.508
B*13:02	1.39	3	0.490
B*14:02	1.39	4	0.315
B*15:01	5.56	10	0.294
B*18:01	5.56	3	0.402
B*27:05	4.17	3	0.680
B*35:01	4.17	6	0.595
B*35:03	4.17	2	0.403
B*38:01	2.78	1	0.379
B*40:01	4.17	2	0.403
B*44:02	4.17	6	0.595
B*49:01	1.39	1	0.814
B*50:01	4.17	1	0.174
B*51:01	15.28	6	0.044
B*52:01	1.39	1	0.814
B*57:01	4.17	2	0.403
C*01:02	4.17	2	0.403
C*02:02	4.17	3	0.680
C*03:03	4.17	11	0.106
C*03:04	6.94	4	0.393
C*04:01	11.11	15	0.460
C*05:01	2.78	5	0.467
C*06:02	13.89	5	0.041
C*07:01	13.89	17	0.580
C*07:02	15.28	12	0.533
C*07:04	1.39	1	0.814
C*08:02	1.39	4	0.315
C*12:02	1.39	1	0.814
C*12:03	5.56	5	0.871
C*15:02	5.56	4	0.632
DRB1*01:01	9.72	7	0.520
DRB1*01:02	1.39	2	0.763
DRB1*03:01	11.11	11	0.982
DRB1*04:01	9.72	3	0.063
DRB1*04:07	1.39	1	0.814
DRB1*04:08	1.39	2	0.763
DRB1*07:01	11.11	12	0.857
DRB1*09:01	1.39	2	0.763
DRB1*11:01	9.72	6	0.363
DRB1*11:03	2.78	2	0.738
DRB1*11:04	1.39	4	0.315
DRB1*12:01	1.39	1	0.814
DRB1*13:01	2.78	10	0.067
DRB1*13:02	2.78	6	0.323
DRB1*15:01	18.06	15	0.592
DRB1*15:02	1.39	1	0.814
DRB1*16:01	1.39	3	0.490
DRB1*01	11.11	9	0.625
DRB1*03	11.11	11	0.956
DRB1*04	15.28	10	0.281
DRB1*07	11.11	12	0.883
DRB1*11	13.89	13	0.838
DRB1*13	5.56	17	0.026
DRB1*15	19.44	16	0.529

Table 4. A. Allele frequencies for (top) presence of *KIR3DL1* gene, (bottom) *KIR3DL1* alleles
(‡) indicates allele not expressed at the cell surface (Guethlein et al., 2015).

B. Genotype frequencies for *KIR3DL1* and *I80⁺HLA-B* in 16th century (plague) and modern inhabitants of Ellwangen. Shown are p values from (chi) chi square, and (lme) logistic mixed effects model.

A

		frequency plague	frequency modern
Gene	<i>KIR3DL1</i>	0.81	0.74
Alleles	<i>*00101</i>	0.25	0.18
	<i>*002</i>	0.17	0.13
	<i>*00401[‡]</i>	0.11	0.08
	<i>*00501</i>	0.13	0.18
	<i>*007</i>	0.03	0.02
	<i>*008</i>	0.07	0.04
	<i>*01502</i>	0.06	0.11

B

	Number Observed				p=	
Genotype	plague (N=36)		modern (N=50)		(chi)	(lme)
<i>I-80⁺HLA-B</i>	20	(55.6%)	16	(32%)	0.029	0.07
<i>KIR3DL1</i>	35	(97.2%)	44	(88%)	0.099	0.29
<i>KIR3DL1 + I-80⁺HLA-B</i>	19	(52.8%)	13	(26%)	0.011	0.01